**ILLUMINA SEQUENCING OF FUNGAL ASSEMBLAGES REVEALS
COMPOSITIONAL SHIFTS AS A RESULT OF NUTRIENT
LOADING WITHIN CAVE SEDIMENTS**

A Thesis
by
BRYAN ZORN

Submitted to the Graduate School
at Appalachian State University
in partial fulfillment of the requirements for the degree of
MASTER OF SCIENCE

August 2014
Department of Biology

ILLUMINA SEQUENCING OF FUNGAL ASSEMBLAGES REVEALS COMPOSITIONAL SHIFTS AS A RESULT OF NUTRIENT LOADING WITHIN CAVE SEDIMENTS

A Thesis
by
BRYAN ZORN
August 2014

APPROVED BY:

_____
Dr. Suzanna L. Bräuer
Chairperson, Thesis Committee

_____
Dr. Sarah K. Carmichael
Member, Thesis Committee

_____
Dr. Ece Karatan
Member, Thesis Committee

_____
Dr. Sue L. Edwards
Biology Department Chairperson

_____
Edelma Huntley
Dean, Cratis Williams Graduate School

Abstract

**ILLUMINA SEQUENCING OF FUNGAL ASSEMBLAGES REVEALS
COMPOSITIONAL SHIFTS AS A RESULT OF NUTRIENT
LOADING WITHIN CAVE SEDIMENTS**

Bryan Thomas Zorn
B.S., Appalachian State University
M.S., Appalachian State University

Chairperson: Dr. Suzanna L. Bräuer

Two geologically comparable epigenic caves in the upper Tennessee River Basin

exhibiting widespread Mn(II) oxidation were used for this study to compare contrasting

hydrologic and nutrient regimes. Using the Illumina MiSeq, fungal ITS1 amplicons were

analyzed to examine baseline community structure as well as phylogenetic shifts as a result

of nutrient loading within the cave sediments. At the phylum level, fungal communities in the

impacted cave had a significantly greater abundance of Ascomycota, suggesting early phase

decomposition of organic matter, whereas those in the near-pristine cave had a greater

abundance of Basidiomycota, suggesting late phase decomposition, and more limited nutrient

input. Corroborating these findings, quantifying the ratios of fungi:bacteria (0.004 ±0.027 of

the impacted cave and 0.007 ±0.069 for the near-pristine cave) were at least an order of

magnitude lower than what is typically reported in soils, which may be attributed to lower

nutrient availability (Carmichael et al., 2013b), dearth of symbionts, or lack of leaf litter

(Baldrian et al., 2012). After exposure to glucose-rich agar casts *in-situ*, Mn oxidation was

subsequently observed, corresponding with a significant increase in the proportion of

Zygomycota as well as a strong increase in cell numbers of bacteria and fungi as determined from qPCR. After nutrient exposure, data revealed an abundance of sequences related to *Mortierella* spp. which only accounted for 1.9% of sequences in the CSPC baseline community. Additionally, one member of this group was cultured, although it is unclear if it is capable of Mn(II) oxidation. Our findings demonstrate that solid exogenous carbon sources can lead to increased production of Mn oxides, increases in bacterial and fungal cell numbers, as well as dramatic changes in fungal assemblages. Further, these results suggest that Mn(II) oxidation is a carbon driven process in these epigenic cave systems.

Acknowledgments

First and foremost, I would like to thank my advisor Dr. Suzanna Bräuer for her constructive suggestions in interpreting and approaching the greater meaning of the data presented in this thesis, as well as its implications on the scientific community and my future directions. I would like to recognize my thesis committee members for helping review and analyze data, providing a professional analytical compass for all information presented in this document. Many thanks are directed towards field members including Kelly Burns and Grey Monroe for sample collection as well as Melanie Hoff and Milton Starnes for guidance and admittance through Carter Salt Peter's Cave and Daniel Boone Caverns, respectively. This research could not have been done without the primary invitation to the project from Leigh-Anne Roble and the patient guidance from Mary-Jane Carmichael throughout the beginning exploratory steps of the project. Cara Santelli, John F. Walker, Chuck Pepe-Ranney, Matt Estep, and Jim Sobieraj helped greatly with essential aspects throughout the experimental process and could not have been completed without their expertise.

Funding this project was made possible by Appalachian State University's Office of Student Research and the Graduate Student Association Senate grants, as well as the North Carolina Space Grant program.

Finally, I would like to thank my parents, David and Lisa Zorn, as well as my siblings for their unending support and respect throughout the years.

Table of Contents

List of Tables

List of Figures

INTRODUCTION

Manganese oxides: crystal structure

Manganese is the second most abundant transition metal in the earth's crust and can exist in a variety of crystallographic phases in nature (Post, 1999). More than 30 Mn oxides have been discovered, and consist of a variety of structures, chemistries, and microscopic and macroscopic morphologies (Post, 1999). The high degree of structural versatility and variability in Mn oxide formation is due to the low energy *d* orbital electrons in Mn, resulting in many stable mineral phases (Matsumoto, 2005).

Manganese can have oxidation states ranging from -3 up to +7, but is generally only observed as +2, +3, and +4 in surface environments (Post, 1999; Trouwborst, Clement, Tebo, Glazer, & Luther, 2006). Overall, Mn(IV) is by far the most dominant valence state in Mn oxides (Manceau, Gorshkov, & Drits, 1992). Although extremely unstable in its unbound form, stable Mn(III) is found to bind with oxyhydrides and –OH groups, and can be complexed with chelating compounds, such as siderophores, and has even been shown to compete with Fe(III) for siderophore binding (Duckworth, Bargar, & Sposito, 2008; Parker, Sposito, & Tebo, 2004). Mn oxide formation can be impacted by a number of factors, such as pH or temperature, and is further influenced by whether the process is biotically or abiotically driven (Post & Bish, 1988; Santelli et al., 2010; Spiro, Bargar, Sposito, & Tebo, 2010; Zhang & Mu, 2007). All Mn oxides, because of their net negativity, possess a staggering capacity to influence their environment by acting as adsorptive traps of heavy

metals and strong oxidizing agents, earning their designation as one of the strongest of natural catalysts (Learman, Voelker, Vazquez-Rodriguez, & Hansel, 2011a; Li & Oyama, 1998; Manceau, Marcus, & Grangeon, 2012; Post, 1999; Tani et al., 2004).

Environmental microcrystalline Mn oxides routinely hold a variable, atypical arrangement of oxidation states, making crystallographic identification difficult even with contemporary techniques and equipment (Manceau et al., 2013; Tebo et al., 2004). Biologically mediated Mn oxides generally take the shape of either layered or tunnel-like structures (Fig. 1) (Tebo et al., 2004).
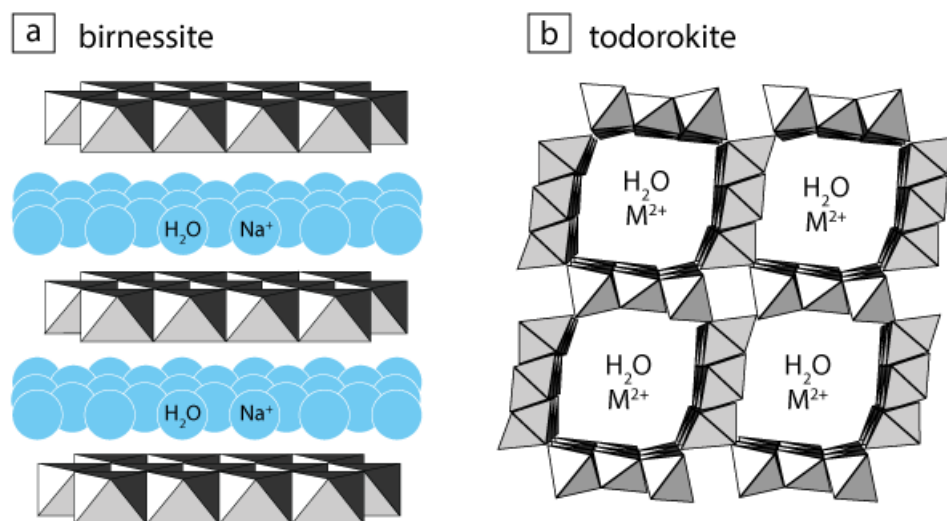

Figure 1. Structures of biogenically mediated Mn oxides (modified from S. K. Carmichael and Bräuer (In review) with permission from the authors). A) Layer-type birnessite. B) Tunnel-type todorokite.

Birnessite (Fig. 1A), a common phyllomanganate found in oceanic and soil Mn nodules, is similar in structure to Mn oxides frequently produced under biotic settings

(Grangeon, Lanson, Miyata, Tani, & Manceau, 2010; Hansel, Zeiner, Santelli, & Webb, 2012; Post, 1999). Birnessite-like phyllomanganates can be characterized as nanocrystalline sheets of 80% Mn(IV), 10% Mn(III), and 10% site vacancies (Manceau et al., 2013). Birnessites contain sheets of Mn octahedra with an approximate interlayer distance of about 7-7.2 Å, although this space can be expanded when fully protonated (Tebo et al., 2004). In this space, the negative charge exerted by the oxide layer is offset most commonly by cations of water and Na+ but may also have cations of aluminum, zinc, or magnesium (Manceau et al., 2012; Manceau et al., 2013; Post, 1999; Post & Veblen, 1990). The mechanism in which metals are incorporated is similar for all Mn oxide structures, where metal and organic ions act as templates during the formation of these minerals, controlling pore size and structure (Feng, Kanoh, & Ooi, 1999; Post, 1999).

Mn oxides such as todorokite (Fig. 1B) form from arrangements of edge-sharing octahedra that form a three dimensional, porous, tunnel-like structure of highly variable size (Manceau et al., 1992; Post, Heaney, & Hanson, 2003). Todorokite is the most common environmental Mn oxide with a tunnel structure and is also found in oceanic Mn oxide nodules, terrestrial Mn ores, and is known to be biologically mediated in some cases (Post, 1999; Santelli, Webb, Dohnalkova, & Hansel, 2011). The structure of todorokite can vary from [3x3] to upwards of [3x9] tunnel regions and has heightened cation concentrations and hydration levels when compared to other tectomanganates (Burns, Burns, & Stockman, 1983; Downs, 2006; Post, 1999).

Microorganisms involved in Mn(II) oxidation

Previous studies have determined that bacteria are likely key producers of microcrystalline Mn oxides (Carmichael, Carmichael, Santelli, Strom, & Bräuer, 2013a; Geszvain et al., 2012; Mann & Quastel, 1946; Parker et al., 2014; Spiro et al., 2010; Tebo et al., 2004), and fungi have recently been documented to take part in the process as well (Carmichael et al., 2013b; Grangeon et al., 2010; Hansel et al., 2012; Miyata, Tani, Iwahori, & Soma, 2004; Santelli et al., 2010). For most phyla, the biological advantage of Mn(II) oxidation is not yet clear. However, the structure, chemistry and reactivity of Mn oxide minerals may provide insight. For example, it has been proposed that due to the high sorption capacity, Mn oxides can be utilized by microorganisms to neutralize aqueous heavy metals that would otherwise be harmful to microorganisms in high concentrations (Santelli et al., 2010). Mn oxides have also been proposed to aid in energy acquisition by degrading recalcitrant carbon sources, such as humic layer acids, into smaller, more bioavailable compounds (Sunda & Kieber, 1994). It has even been asserted that Mn oxides can serve as protective shields for bacteria by forming an intense redox barrier, debilitating foreign surface proteins, and by serving as a barrier against other microorganisms and viruses (Tebo et al., 2004). Interestingly, no study to date has incontrovertibly demonstrated a physiological function or benefit of bacterial Mn(II) oxidation, although some evidence suggests that Mn(II) oxidation in some bacteria may simply be a side-effect of other cellular processes (Learman et al., 2011a).

Bacterial Mn(II)-oxidizers have been identified in a variety of environments, ranging from terrestrial soils (Tebo, Johnson, McCarthy, & Templeton, 2005; Villalobos, Lanson, Manceau, Toner, & Sposito, 2006), desert varnishes (Grote & Krumbein, 1992), estuaries

(Bräuer et al., 2011; Lauber, Strickland, Bradford, & Fierer, 2008), caves (Cunningham, Northup, Pollastro, Wright, & LaRock, 1995; Northup et al., 2000), marine sediments (Davis & Tebo, 2013) and seamounts (Templeton, Staudigel, & Tebo, 2005). Mn(II)-oxidizing fungal strains have been isolated from terrestrial soils and desert varnishes (Grote & Krumbein, 1992), acid mine drainage sites (Santelli et al., 2010), freshwater streams (Grangeon et al., 2010), caves (Bastian, Jurado, Novakova, Albouvette, & Saiz-Jimenez, 2010; Carmichael et al., 2013b), and even man-made structures (Delatorre & Gomezalarcon, 1994). Members of the fungal kingdom that are known to oxidize Mn belong to genera *Phoma, Pithomyces, Pyrenchaeta, Stagonospora, Plectosphaerella, Microdochium, Stibella, Alternaria, Paraconiothyrium,* and *Acremonium*, but other fungi may be covert contributors to this biogeochemical process as well (Santelli et al., 2011; Tang, Zeiner, Santelli, & Hansel, 2013). Basidomycota and Ascomycota are typically the dominant fungal phyla recovered from DNA-based soil surveys (Buee et al., 2009; O'Brien, Parrent, Jackson, Moncalvo, & Vilgalys, 2005; Schadt, Martin, Lipson, & Schmidt, 2003; Schmidt et al., 2013), and members of both phyla have been recognized to oxidize Mn(II). Ascomycete fungi typically produce hexagonal and triclinic birnessite and buserite and less commonly todorokite (Santelli et al., 2011; Tebo et al., 2005). Although not as frequently produced, todorokite can form exclusively on solid media from certain strains (Santelli et al., 2011), but may simply be an abiotic derivative from the topotactic collapse of phyllomanganate structures such as birnessite (Bodei, Manceau, Geoffroy, Baronnet, & Buatier, 2007; Grangeon et al., 2010; Santelli et al., 2011).

Biological mechanisms of Mn(II) oxidation

Oxidation of Mn(II) is thermodynamically unfavorable under typical environmental conditions, but these reactions do become favorable in the presence of certain biological catalysts (Luther, 2010). Two biotic pathways, enzymatic (Webb, Dick, Bargar, & Tebo, 2005) and/or superoxide routes (Hansel et al., 2012; Learman et al., 2011a), have been postulated to be associated with the production of Mn oxides. The major enzymatic pathway involves multicopper oxidase (MCO)-type proteins that function by removing an electron from the substrate (in this case a soluble Mn(II) ion) and shuttling that electron from the type I site to the type III site, ultimately reducing diatomic oxygen into water (Geszvain et al., 2012). Members of Basidomycota in particular may possess many variants of multicopper oxidase family-like proteins, such as laccases, which contribute to useful biocatalytic properties such as the degradation of lignin (Tamayo-Ramos, van Berkel, & de Graaff, 2012). These oxidases are a large group of enzymes with cross-domain homologues which are lax in their specificity for reducing substrates (Kosman, 2010). The enzymes also contain three binding site types of copper complexes, all of which work in similar ways to efficiently oxidize aromatic amines, cyclic polyols, acids, and metals such as Fe, Cu, and Mn (Kosman, 2010). MCO-type proteins can be found in bacteria that oxidize Mn, such as *Aurantimonas manganoxydans* SI85-9A1 and *Erythrobacter* sp. SD-21 (Anderson et al., 2009), *Leptothrix discophora* SS-1 (Corstjens, de Vrind, Goosen, & de Vrind-de Jong, 1997), *Pedomicrobium* sp. ACM 3067 (Larsen, Sly, & McEwan, 1999), and *Bacillus* sp. (Mayhew, Swanner, Martin, & Templeton, 2008). Recent research indicates that some bacteria may possess multiple Mn(II)-oxidizing MCO genes, as *P. putida* required the knockout of two putative Mn oxidase genes, in order to inhibit Mn oxide synthesis (Geszvain, McCarthy, & Tebo, 2013). Further,

genome analysis has identified other strains that carry multiple putative Mn oxidases (Davis & Tebo, 2013).

Another more indirect method of Mn(II) oxidation involves superoxide production by NADPH oxidases. The NADPH oxidase (NOX) protein complex is dedicated to generation of reactive oxygen species and is in general made up of six subunit domains: NOX1-5, and DUOX1/2, which are all found to have homologues across eukaryotic kingdoms (Aguirre, Rios-Momberg, Hewitt, & Hansberg, 2005; Bedard & Krause, 2007). In order for the complex to become activated, the cytosolic regulatory protein complex made up of $p40^{phox}$, $p67^{phox}$, and $p47^{phox}$ must be phosphorylated at the $ph47^{phox}$ subunit. Once phosphorylated, a conformational change allows binding with $p22^{phox}$ (cytochrome b-245 alpha polypeptide), a NOX2 (also named as $gp91^{phox}$ and cytochrome b-245, beta polypeptide) associated protein to form flavocytochrome b_{558} containing FAD (Bedard & Krause, 2007; Lambeth, 2004). Once bound to flavocytochrome b_{558}, NOX2 is then capable to interact with independently generated GTP Rac (Heyworth, Bohl, Bokoch, & Curnutte, 1994; Lambeth, 2004). Once fully activated and incorporated within the phospholipid bilayer, the metacomplex of flavocytochrome b_{558} and associated NOX proteins, phosphorylated cystolic regulatory complex, and GTP Rac catalyzes a two-step electron transfer (Bedard & Krause, 2007). The first step of the process is the transfer of electrons from NADPH + H^+, potentially as arachidonic acid, to FAD, generating $FADH_2$ which then favorably donates a single electron to the most interiorly located heme A (Bedard & Krause, 2007; Vignais, 2002). The subsequent transfer between heme groups, which alone is unfavorable, is overcome by the ambient oxidation of outer heme B by diatomic oxygen which in turn generates a superoxide O_2^- (Vignais, 2002). Vignals (2002) has summarized the net reaction presented below:

$$NADPH + 2O_2 \rightarrow NADP^+ + H^+ + 2O_2^-$$

The external superoxide product is independent of dismutase proteins and among other reactants, can react with metals such as Mn(II) to form a Mn(III) biointermediate (Aguirre et al., 2005; Lambeth, 2004; Learman et al., 2011b; Santelli et al., 2010). Many reactive oxygen species, including hydrogen peroxide, superoxide and hydroxyl radicals are predicted to be favorable oxidants for catalyzing Mn(II) oxidation at environmentally and biologically relevant pHs (Luther, 2010). The NADPH oxidase protein family is thereby thought to mediate oxidation of Mn(II) through a respiratory burst of superoxide that is produced upon cell division, pathogenic invasion, or differentiation (Giesbert, Schurg, Scheele, & Tudzynski, 2008; Hansel et al., 2012; Takemoto, Tanaka, & Scott, 2007). For example, when *Pyrenchaeta* sp. DS3sAY3a and *Stagonospora* sp. SRC1lsM3a fungal species were cultured with NADPH inhibitors or high Cu(II) concentrations that outcompete Mn(II) for oxidation by superoxide, Mn(II) oxidation was greatly inhibited (Tang et al., 2013).

Siderophore mediated Mn(II) oxidation in both bacteria and fungi

Siderophores, which have high affinities to iron, manganese, and other metals, are also thought to mediate Mn(II) oxidation by chelating and solubilizing these ions into forms that can be further oxidized (Braud, Hoegy, Jezequel, Lebeau, & Schalk, 2009; Neilands, 1995; Webb et al., 2005). Pyoverdine, for example, has been observed as a definitive Mn(III)-complexed intermediate in a bacterial model of Mn(II) oxidation, and is also predicted to have homologues across other kingdoms (Parker et al., 2004). Characteristically similar ligands produced in fungi, such as oxalic, citric, and hydroxamic acids and their

derivatives are reported to have strong chelating affinities with iron and have also been observed to sequester extracellular Mn(III) as well (Gadd, 1999; Holzberg & Artis, 1983). Mn(IV) oxide precipitates can be found in close association with bacterial and fungal cells, suggesting that membrane-bound siderophores may mediate the formation of some biogenic Mn(IV) oxides (Santelli et al., 2011; Tang et al., 2013).

Manganese oxides within cave systems

Cave environments are geographically widespread and are unique and important ecosystems (White, Culver, Herman, Kane, & Mylroie, 1995). Within these systems, ferromanganese oxide crust layers have been shown to potentially contribute to trace element and nutrient biogeochemical cycling, and are thought to be predominantly of bacterial and fungal origin (Carmichael et al., 2013a; Carmichael et al., 2013b; Northup et al., 2003; Spilde et al., 2005; White, Vito, & Scheetz, 2009). Bacterial communities associated with ferromanganese oxide deposits within cave systems have been shown to be quite diverse (Carmichael et al., 2013a), however, our understanding of the microorganisms involved remains incomplete as the geomicrobiological contributions of Mn(II) oxidizing fungi have been long overlooked. Thus, it is important to obtain a full community profile of the microbial consortia including fungi in ferromanganese oxide deposits. Next generation sequencing such as the Illumina platform offer numerous benefits over traditional sequencing techniques, but has generally focused on the bacterial kingdom (Caporaso et al., 2012). However, recent studies have shown it can be used reliably for determining fungal community structure using internal transcribed spacer (ITS) amplicons (Anderson et al., 2009; Schmidt et al., 2013). To the best of our knowledge, this thesis is the first study to

utilize the Illumina sequencing platform in the analysis of fungal communities associated with cave ferromanganese oxide deposits. Herein, the phylogenetic relationships of the microorganisms within these communities is assessed and compared to other soil communities. This work not only provides useful information to how cave ferromanganese oxide deposits may evolve, but also proposes a mechanism for how these unique and fragile ecosystems can be monitored and maintained.

MATERIALS AND METHODS

Field Description

Two comparable epigenic caves in the upper Tennessee River Basin were used for this study to compare contrasting nutrient regimes. Both caves are located within the Ordovician Knox Dolomite Group, and experience nearly identical climate and rainfall patterns. The anthropogenically impacted study sites were located within Carter Saltpeter Cave in Carter County, TN, USA (Fig. 2A), herein referred to as CSPC. CSPC is a shallow, epigenic cave system typical of the southern Appalachian region, and evidence of anthropogenic impact is widespread throughout the cave in the form of trash, sewage, and debris (Carmichael et al., 2013a; Carmichael et al., 2013b). There are many active seeps and a large lake in the middle of the cave, and it is highly susceptible to flooding. The near-pristine study sites were located within Daniel Boone Caverns (herein referred to as DBC) in Scott County, VA (Fig. 2B). DBC is a gated and rarely-visited cave where access is controlled by the landowner. It is located in an isolated forest on the top of a ridge and therefore is not subject to flooding or agricultural or municipal runoff. It contains several pools and drip networks, but does not have an extensive subsurface hydrologic system. These pools and drip networks in DBC show no geochemical evidence of anthropogenic impact nor elevated nutrient levels (Carmichael et al., 2013b), thereby justifying its use as a pristine analogue of CSPC.
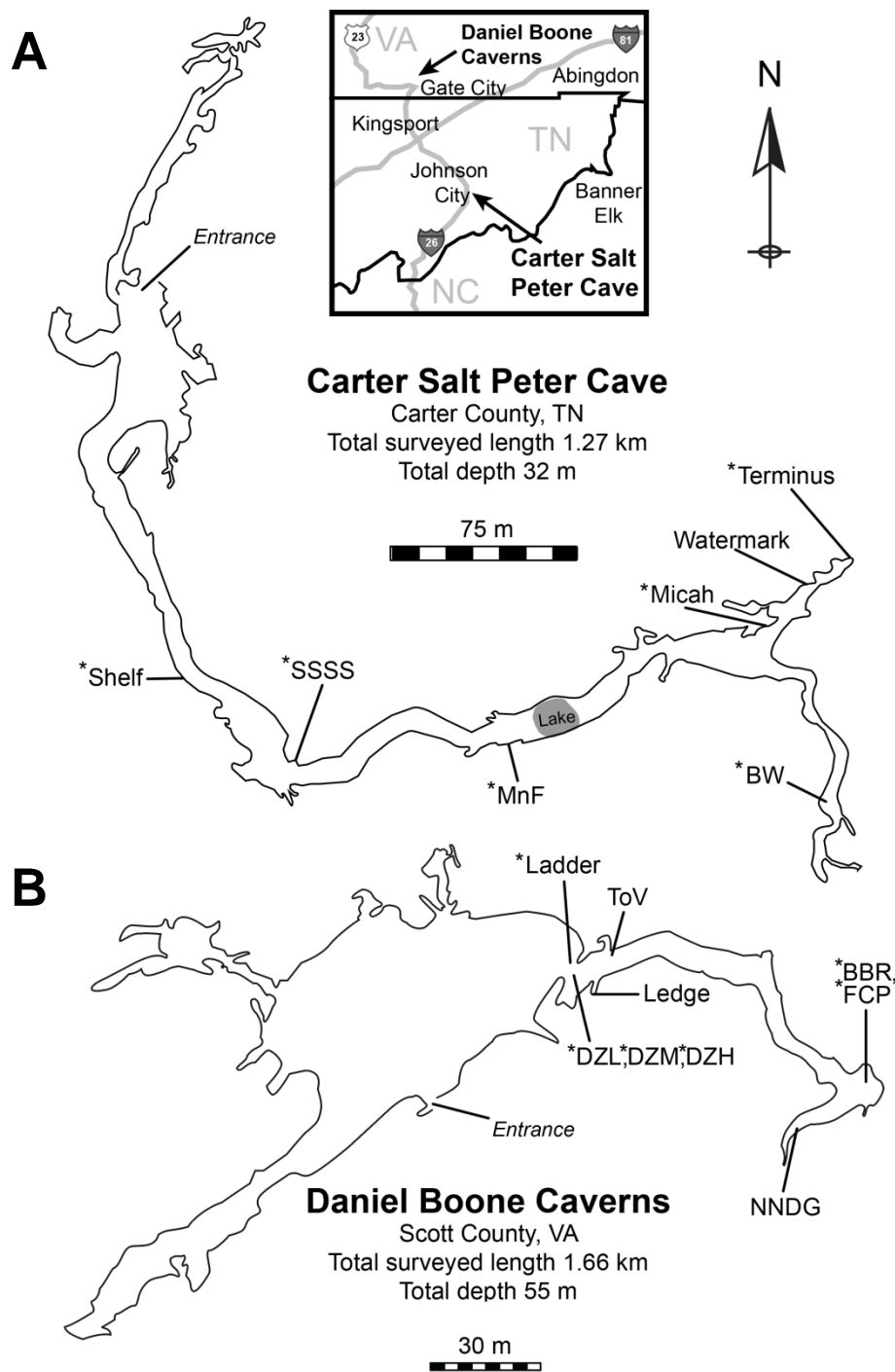
Figure 2. Location, maps and sampling locations within Carter Saltpeter Cave (CSPC) and Daniel Boone Caverns (DBC). Asterisks denote nutrient supplementation sites. Cave survey of CSPC conducted on February 8, 1981 by L. Adams, R. Knight, R. Page, and T. Wilson. Cave map drafted by L. Adams and adapted by S. Carmichael. Initial cave survey of Daniel Boone Caverns conducted in 1969 by M. Starnes, B. Lucas, D. Breeding, C. Stowers, and B. Balfour, and an additional survey was conducted from July-November 1996. Two substantial passages in the cave have not yet been surveyed. Cave maps adapted by B. T. Zorn, 2014.

Sample collection

During September-October 2012, sample substrates within CSPC and DBC were screened *in situ* for the presence of Mn(III/IV) oxides using Leucoberbelin blue indicator dye. Sampling sites that produced a deep blue reaction were collected, stored on ice and transported to the laboratory for processing within 2.5 hours. Samples were partitioned for culturing efforts and stored under refrigeration while approximately 500 mg of substrate from each site was used for DNA extraction following the manufacturer's protocols using the FastDNA^{TM} SPIN Kit for Soil (MP Biomedicals, LLC. Solon, OH, USA). DNA was stored under -20°C for subsequent usage.

Real-time quantitative PCR

Twenty-four samples across two cave systems were analyzed using real-time quantitative PCR to estimate the relative abundance of bacteria and fungi in CPSC and DBC. Primers were selected for each domain demonstrating broad coverage over bacterial 16S rRNA and fungal ITS1 regions. The bacterial forward primer 338F 5'TCC TACGGGAGGCAGCAGT (Nadkarni, Martin, Jaques, & Hunter, 2002) was paired with the reverse primer 5.18R 5'ATTACCGCGGCTGCTGG (Einen, Thorseth, & Ovreas, 2008) to target the SSU rRNA gene sequence (Johnson et al., 2012). The fungal ITS1 gene sequence was targeted using the ITS1F 5'TCCGTAGGTGAACCTGCGG and 5.8SR 5'CGCTGCGTTCTTCATCG primer pair (Fierer, Jackson, Vilgalys, & Jackson, 2005). Standard calibration curves for quantification were generated from plasmid DNA containing either a bacterial SSU rRNA gene sequence (range of 10^2–10^9 target copies/µL) from *Rhodobacter* sp. CR07-74 (Bräuer et al., 2011); or a fungal rRNA ITS1 gene sequence from

Saccharomyces cerevisiae (range of 10^2-10^8 target copies/µL). Plasmid DNA standards were linearized by restriction digest using either BssHII for the bacterial or NCOI-HF[TM] for the fungal plasmid (New England BioLabs, Ipswich, MA, USA). DNA was amplified in 25 uL reaction volumes in triplicate under optically transparent sealing films on an Applied Biosystems[TM] 7300 Real-Time PCR System (Carlsbad, CA, USA) using 12.5 µL of GoTaq® qPCR Master Mix (Promega Corporation, Fitchburg, WI), 2.5 µL of each forward and reverse primer (10 µM initial concentrations), 0.25 µL of BSA (New England Biolabs, Ipswich, MA, USA), 6.75 µL nuclease free water, and 1 µL of DNA at two different concentrations to control for PCR inhibition. Thermocycling conditions for bacterial amplification began with 50°C for 2 minutes and 95°C for 10 minutes, followed by 39 cycles of 95°C for 15 seconds, 60°C for 1 minute, and ending with a final dissociation consisting of 95°C for 15 seconds. Fungal thermocycling was performed at 95°C for 15 minutes, followed by 40 cycles at 95°C for 1 minute, 53°C for 30 seconds, 72°C for 1 minute, and ending with a final dissociation of 95°C for 15 seconds. Data analyses were performed using Applied Biosystems 7300 System SDS Software version 1.3.1.21.

rRNA operon copy numbers in microbial cells are variable (Fogel, Collins, Li, & Brunk, 1999; Warner, 1999) and change based on environmental conditions (Klappenbach, Dunbar, & Schmidt, 2000; Anderson & Cairney, 2004). Therefore, SSU rRNA gene copy number was normalized using the average copy number per cell. For bacteria, 4.08 copies per cell were used as reported by the Ribosomal RNA Operon Copy Number Database in April 2010 (Klappenbach, Saxman, Cole, & Schmidt, 2001). Fungal amplicons were normalized to 150 copies of ribosomal RNA gene operons per cell, as quantities have been found to vary

greatly between fungal lineages as well as for cells in various stages of ploidy (Vilgalys &

Gonzalez, 1989; Longo et al., 2013; Zhang et al., 2013).

Amplification and sequencing

The ITS1f primer 5'TCCGTAGGTGAACCTGCGG was modified from Gardes and

Bruns (1993) with the addition of: 1) the reverse compliment of the Illumina adapter

5'CAAGCAGAAGACGGCATACGAGAT), 2) a twelve base pair unique Golay barcode

distinguishing sample site, 3) reverse primer pad of 5'AGTCAGTCAG, and 5'CC linker, all

attached to the 5' end of ITS1f according to the design of J. G. Caporaso et al. (2012; Table

1).

Similarly, the 5.8s reverse primer 5'CGCTGCGTTCTTCATCG was modified from

Vilgalys and Hester (1990) with the addition of: 1) the Illumina adapter

5'AATGATACGGCCACCACCAGATTACAC, 2) forward primer pad 5'TATGGTAATT,

3) primer linker 5'GT, all attached to the 5' end of the 5.8s reverse as described by J. G.

Caporaso et al. (2012). Each 25 μL reaction mixture consisted of 12.5 μL of Q5® Hot Start

High-Fidelity DNA Polymerase (New England Biolabs, Ipswich, MA, USA), 2.5 μL of

modified forward and reverse primers, 0.25 μL of BSA (New England Biolabs, Inc. Ipswich,

MA, USA), 6.75 μL nuclease free water, and 1 μL of DNA. Amplification was carried out in

triplicate for twenty-four DNA samples on the MJ Mini[TM] Personal Thermocycler (Bio-Rad

Laboratories. Hercules, CA, USA) using a touchdown PCR protocol. Thermocycler reactions

included 95°C for 10 minutes, followed by 10 touchdown cycles at 94°C for 45 seconds,

68°C to 58°C (decrease of 1°C per cycle) for 45 seconds, followed by extension at 72°C for

75 seconds. An additional 27 cycles followed with 95°C for 45 seconds, 58°C for 45 seconds

and a final additional extension of 72°C for 10 minutes. For sites producing lower band

intensity, this additional step was increased to 29 cycles. Amplified DNA was stained using GelRed (Phenix Research. Asheville, NC, USA) and separated in 1X TAE buffered, 1% agarose gel at 35 volts for approximately 1 hour with Amresco UV fluorescent loading dye.

PCR products were purified from the electrophoresis gel and normalized to an even concentration. The processed sample was determined to have an average amplicon size of 360 base pairs, ranging from 250 to 500 base pairs, and was shipped to West Virginia University's Genomics Core Facility (Morgantown, WV, USA) for paired-end sequencing on a MiSeq sequencer (Illumina, Inc. San Diego, CA, USA). All raw sequence reads were submitted to the European Nucleotide Archive (Leinonen et al., 2010) under the primary accession number PRJEB6581.

Table 1. Forward sequencing amplification primers. Each primer name was assigned to a sample site and thereby later identified using its Golay barcode. Each primer is made up of five specific parts starting from the 1) reverse compliment of the 3' Illumina adapter attached to the 2) Golay barcode attached to the 3) reverse primer pad and 4) linker ending with the 5) ITS1f primer sequence.

Primer Name	Reverse compliment of the Illumina 3' adapter	Golay Barcode	Reverse primer pad	Reverse linker	ITS1F primer sequence
ITS108	CAAGCAGAAGACGGCATACGAGAT	GCACACCTGATA	AGTCAGTCAG	CC	TCCGTAGGTGAACCTGCGG
ITS109	CAAGCAGAAGACGGCATACGAGAT	GCGACAATTACA	AGTCAGTCAG	CC	TCCGTAGGTGAACCTGCGG
ITS110	CAAGCAGAAGACGGCATACGAGAT	TCATGCTCCATT	AGTCAGTCAG	CC	TCCGTAGGTGAACCTGCGG
ITS111	CAAGCAGAAGACGGCATACGAGAT	AGCTGTCAAGCT	AGTCAGTCAG	CC	TCCGTAGGTGAACCTGCGG
ITS112	CAAGCAGAAGACGGCATACGAGAT	GAGAGCAACAGA	AGTCAGTCAG	CC	TCCGTAGGTGAACCTGCGG
ITS113	CAAGCAGAAGACGGCATACGAGAT	TACTCGGGAACT	AGTCAGTCAG	CC	TCCGTAGGTGAACCTGCGG
ITS114	CAAGCAGAAGACGGCATACGAGAT	CGTGCTTAGGCT	AGTCAGTCAG	CC	TCCGTAGGTGAACCTGCGG
ITS115	CAAGCAGAAGACGGCATACGAGAT	TACCGAAGGTAT	AGTCAGTCAG	CC	TCCGTAGGTGAACCTGCGG
ITS116	CAAGCAGAAGACGGCATACGAGAT	CACTCATCATTC	AGTCAGTCAG	CC	TCCGTAGGTGAACCTGCGG
ITS117	CAAGCAGAAGACGGCATACGAGAT	GTATTTCGGACG	AGTCAGTCAG	CC	TCCGTAGGTGAACCTGCGG
ITS118	CAAGCAGAAGACGGCATACGAGAT	TATCTATCCTGC	AGTCAGTCAG	CC	TCCGTAGGTGAACCTGCGG
ITS119	CAAGCAGAAGACGGCATACGAGAT	TTGCCAAGAGTC	AGTCAGTCAG	CC	TCCGTAGGTGAACCTGCGG
ITS120	CAAGCAGAAGACGGCATACGAGAT	AGTAGCGGAAGA	AGTCAGTCAG	CC	TCCGTAGGTGAACCTGCGG
ITS121	CAAGCAGAAGACGGCATACGAGAT	GCAATTAGGTAC	AGTCAGTCAG	CC	TCCGTAGGTGAACCTGCGG
ITS122	CAAGCAGAAGACGGCATACGAGAT	CATACCGTGAGT	AGTCAGTCAG	CC	TCCGTAGGTGAACCTGCGG
ITS123	CAAGCAGAAGACGGCATACGAGAT	ATGTGTGTAGAC	AGTCAGTCAG	CC	TCCGTAGGTGAACCTGCGG
ITS124	CAAGCAGAAGACGGCATACGAGAT	CCTGCGAAGTAT	AGTCAGTCAG	CC	TCCGTAGGTGAACCTGCGG
ITS125	CAAGCAGAAGACGGCATACGAGAT	TTCTCTCGACAT	AGTCAGTCAG	CC	TCCGTAGGTGAACCTGCGG
ITS126	CAAGCAGAAGACGGCATACGAGAT	GCTCTCCGTAGA	AGTCAGTCAG	CC	TCCGTAGGTGAACCTGCGG
ITS127	CAAGCAGAAGACGGCATACGAGAT	GTTAAGCTGACC	AGTCAGTCAG	CC	TCCGTAGGTGAACCTGCGG
ITS128	CAAGCAGAAGACGGCATACGAGAT	ATGCCATGCCGT	AGTCAGTCAG	CC	TCCGTAGGTGAACCTGCGG
ITS129	CAAGCAGAAGACGGCATACGAGAT	GACATTGTCACG	AGTCAGTCAG	CC	TCCGTAGGTGAACCTGCGG
ITS130	CAAGCAGAAGACGGCATACGAGAT	GCCAACAACCAT	AGTCAGTCAG	CC	TCCGTAGGTGAACCTGCGG
ITS131	CAAGCAGAAGACGGCATACGAGAT	ATCAGTACTAGG	AGTCAGTCAG	CC	TCCGTAGGTGAACCTGCGG

Data processing

MOTHUR was used to assemble and trim contigs after discarding sequences
containing nucleotide ambiguities and regions with <11 homopolymers (Schloss et al., 2009).
Chimeric sequences were identified *de novo* within QIIME using USEARCH6.1 and
subsequently removed from the working data set (Caporaso et al., 2011; Edgar, Haas,
Clemente, Quince, & Knight, 2011). Operational taxonomic units (OTUs) were clustered
within QIIME at a 97% similarity. Classification of OTUs employed the BLAST (Altschul,
Gish, Miller, Myers, & Lipman, 1990) algorithm through QIIME against the publicly
available UNITE reference database (Version No. 6, Release date 2014-01-15) (Altschul et
al., 1990; Koljalg et al., 2005; Abarenkov et al., 2010). All other additional diversity analyses
were performed within QIIME version 1.7.0 under non-phylogentic constraints (Caporaso et
al., 2011).

In-situ **enrichment**

During sample collection, agar media casts were applied to six locations within CSPC
(Shelf, SSSS, MnF, Micah, BW, and Terminus) and six sites within DBC on October 2012,
(MSW, DZL, DZM, DZH, BBR, and FCP; Fig. 2). Each location received a single set of agar
casts consisting of one or more of the following media types: 1) glucose media: containing
40 g L^{-1} dextrose, 10 g L^{-1} peptone, 20 g L^{-1} agar; 2) AY medium (Santelli et al 2010); 3)
malt medium: 20 g L^{-1} malt extract, 20 g L^{-1} agarose; 4) nitrate medium: 5 g L^{-1} peptone, 3 g
L^{-1} meat extract, 1 g L^{-1} KNO$_3$, 18 g L^{-1} agar; 5) citrate medium: 2.5 g L^{-1} NaCl, 2 g L^{-1}
sodium citrate, 1 g L^{-1} ammonium sulfate, 15 g L^{-1} agar. All media were supplemented with
the following ingredients (filter sterilized and added after autoclaving): 100 μM MnCl$_2$ and 1

mL per liter trace elements (10 mg L^{-1} $CuSO_4$ ·$5H_2O$, 44 mg L^{-1} $ZnSO_4$ ·$7H_2O$, 20 mg L^{-1} $CoCl_2$ ·$6H_2O$, 13 mg L^{-1} Na_2MoO_4 ·$2H_2O$), (Santelli et al., 2011). During a period of two months, the glucose agar cast at Terminus in CSPC became initially colonized by white fungal mycelia (Fig. 3A), and then turned dark brown (Fig. 3B). After ca. ten weeks of incubation, on November 15, 2012, Terminus and SSSS showed a strong stimulation of Mn(II) oxidation, while another site, MnF, demonstrated weak stimulation according to field observations and LBB reactions (Fig 3B, 3C). Thus, these three sites were used for enrichment studies as other sites showed no significant evidence of colonization or Mn(II) oxidation. None of the sites in DBC showed any reaction within the timeframe of this study. Duplicate samples from each of these three sites were collected for DNA extraction in order to quantify abundance and to evaluate potential shifts in fungal assemblages. Additionally, partitioned sediment from field collections was diluted with sterile distilled H_2O and spread onto culture media less than 48 hours after collection in an attempt to isolate fungi exhibiting Mn(III/IV) oxide production. After fungal cultures were deemed pure and identified as Mn(II)-oxidizing, they were sent to Dr. Cara Santelli at the Smithsonian Institution's National Museum of Natural History for verification of purity as well as sequencing of the fungal SSU, ITS1, and LSU rRNA genes.
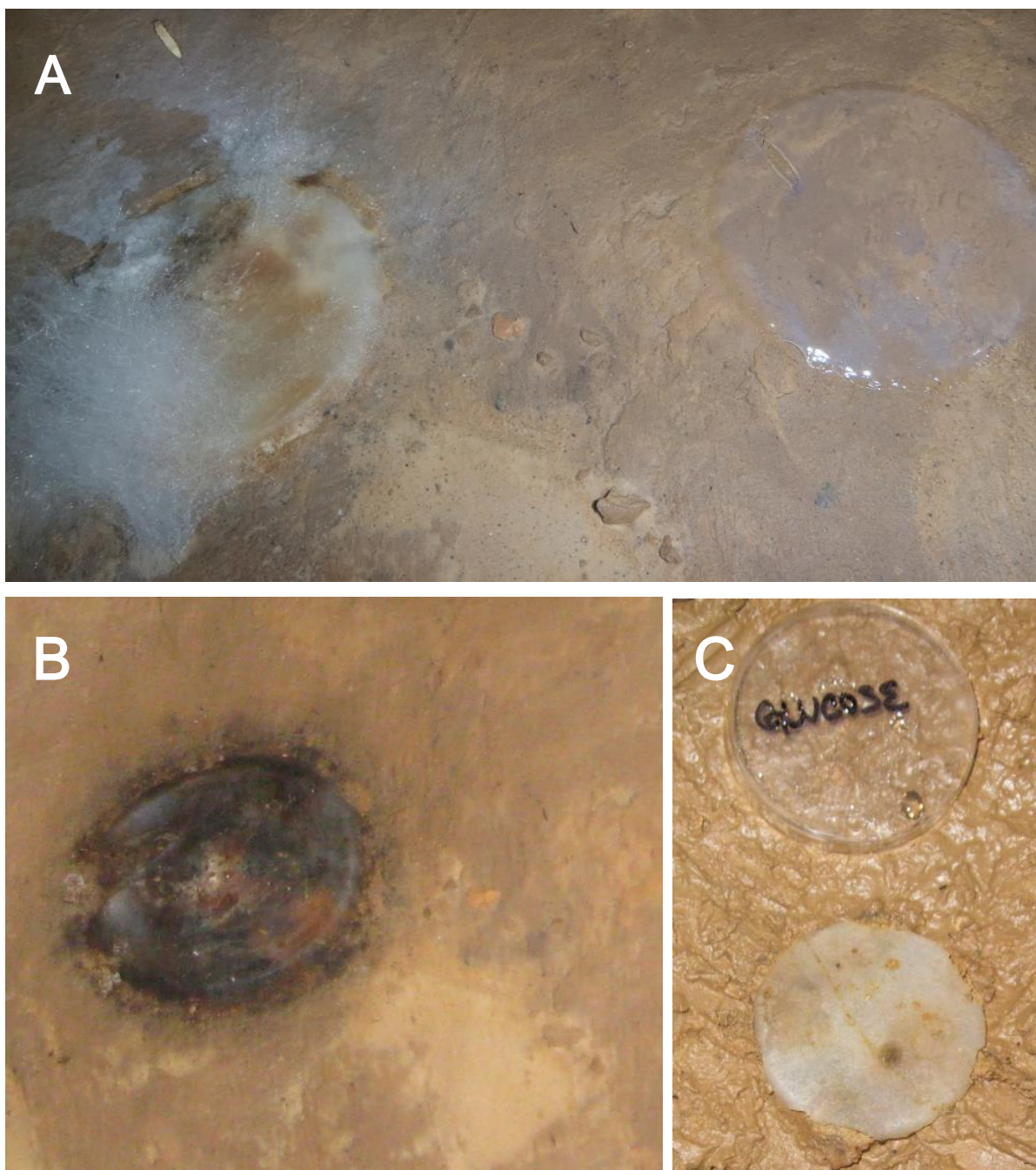
Figure 3. Fungal colonization of media casts *in-situ*. (A) Aerial hyphae colonizing glucose media in CSPC at site Terminus. (B) Approximately two weeks after fungal colonization, characteristic brown-black LBB positive sediment in, on, and around the agar cast. (C) Glucose media at site MnF showing weak Mn(II) oxidation.

RESULTS

Real-time qPCR of baseline communities

Standard curves for bacterial qPCR runs produced R^2 value of 0.99 with an estimated amplification efficiency of 103%. Standard curves from fungal runs produced R^2 value of 0.98 and and estimated amplification efficiency of 110%. The estimated number of fungal cells represented a small percentage of the microbial community as measured on a per cell basis, with fungal:bacterial ratios of 0.00009:1 and 0.00008:1 for CSPC and DBC, respectively. Bacterial SSU rRNA gene quantification resulted in an estimated 6.37×10^7 - 4.10×10^9 cells per gram wet weight within CSPC whereas DBC was estimated to contain significantly fewer ($P = 0.007$) bacterial cells, ranging from 1.03×10^7 - 7.38×10^8 cells per gram wet weight (Fig. 4). Quantification of fungal ITS1 region amplicons within CSPC yielded an estimated 1.62×10^4 - 3.96×10^5 cells per gram wet weight while fungal cell approximations were significantly lower ($P = 0.012$) and varied more widely within DBC representing 1.20×10^2 - 5.89×10^4 cells per gram wet weight.
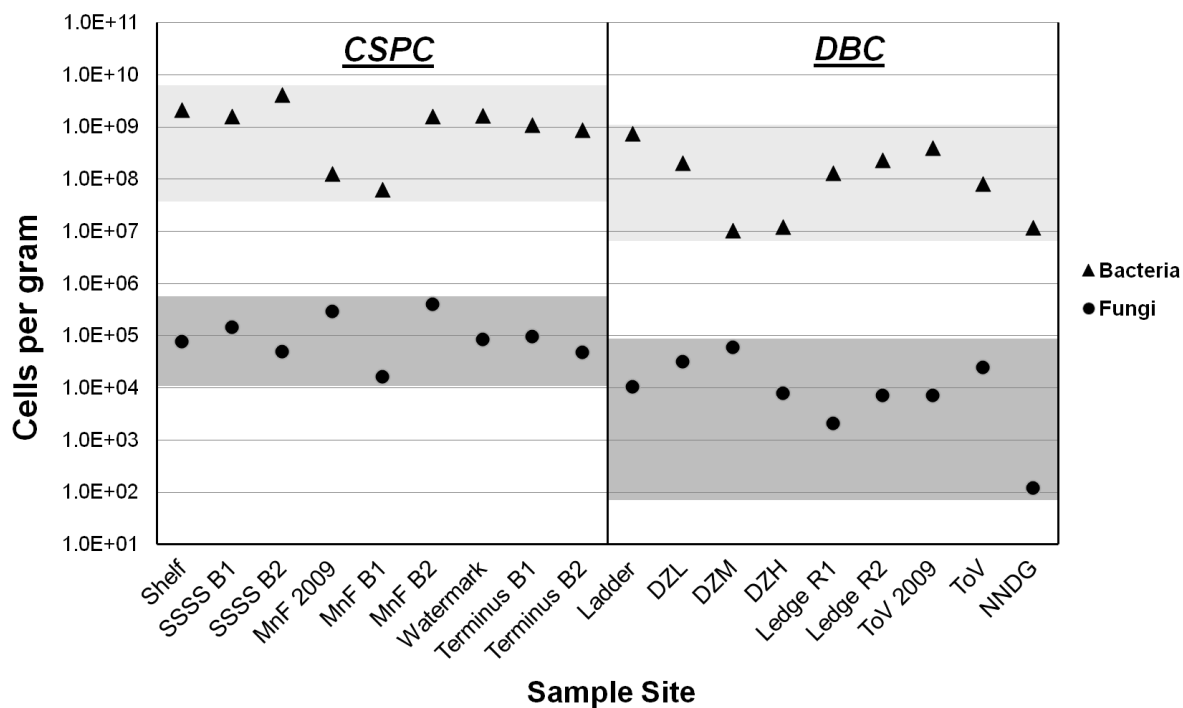
Figure 4. Estimated number of bacterial (light shade) and fungal (dark shade) cells per gram wet weight. Cell abundance was estimated from real-time qPCR of the SSU rRNA gene for bacteria or the ITS1 region for fungi.

Phylogenetic analysis of baseline fungal communities

After processing, roughly 470,000 sequences were distributed among 877 unique OTUs. Using this data set, a significant difference between alpha diversity ($P < 0.05$) was found between cave samples across all metrics tested (Table 2).

Abundance-weighted Jaccard principal coordinate analyses were conducted in order to determine beta diversity among fungal OTUs. In three dimensional PCoA under abundance-weighted Jaccard, samples within each cave tended to cluster together and clear separation between cave samples was observed (Fig. 5).

Table 2. Alpha diversity estimates for samples from CSPC and DBC across multiple diversity indices, including ACE, Chao1, Simpson, Shannon, and Observed Species. Average values for each cave as well as P-value results from a T-TEST comparison between cave samples is shown for each metric. A significant P value is denoted by an asterisk (*).

|		ACE	Chao1	Simpson	Shannon	Observed Species
CSPC						
Shelf		479.63	467.96	0.95	5.74	444
SSSS B1		524.04	521.28	0.97	6.54	482
SSSS B2		520.65	525.93	0.96	5.87	456
MnF 2009		104.56	102.33	0.55	2.72	61
MnF B1		54.74	49.00	0.70	2.57	44
MnF B2		145.03	130.25	0.84	3.13	107
Watermark		214.65	211.26	0.97	5.94	196
Terminus B1		205.46	203.25	0.94	5.02	186
Terminus B2		302.50	278.44	0.93	5.20	244
	Average	283.47	276.63	0.87	4.75	246
DBC						
Ladder		81.24	71.00	0.55	1.93	61
DZL		101.07	95.00	0.61	2.48	72
DZM		203.44	120.50	0.90	4.22	43
DZT		172.04	122.60	0.81	3.43	56
Ledge R1		95.44	104.00	0.92	4.33	70
Ledge R2		153.99	133.50	0.79	3.42	102
ToV 2009		135.47	98.17	0.63	1.84	44
ToV		75.58	65.60	0.69	2.48	35
NNDG		81.47	78.27	0.79	2.74	51
	Average	122.19	98.74	0.74	2.99	59
	P-value	**0.015***	**0.010***	**0.040***	**0.005***	**0.006***
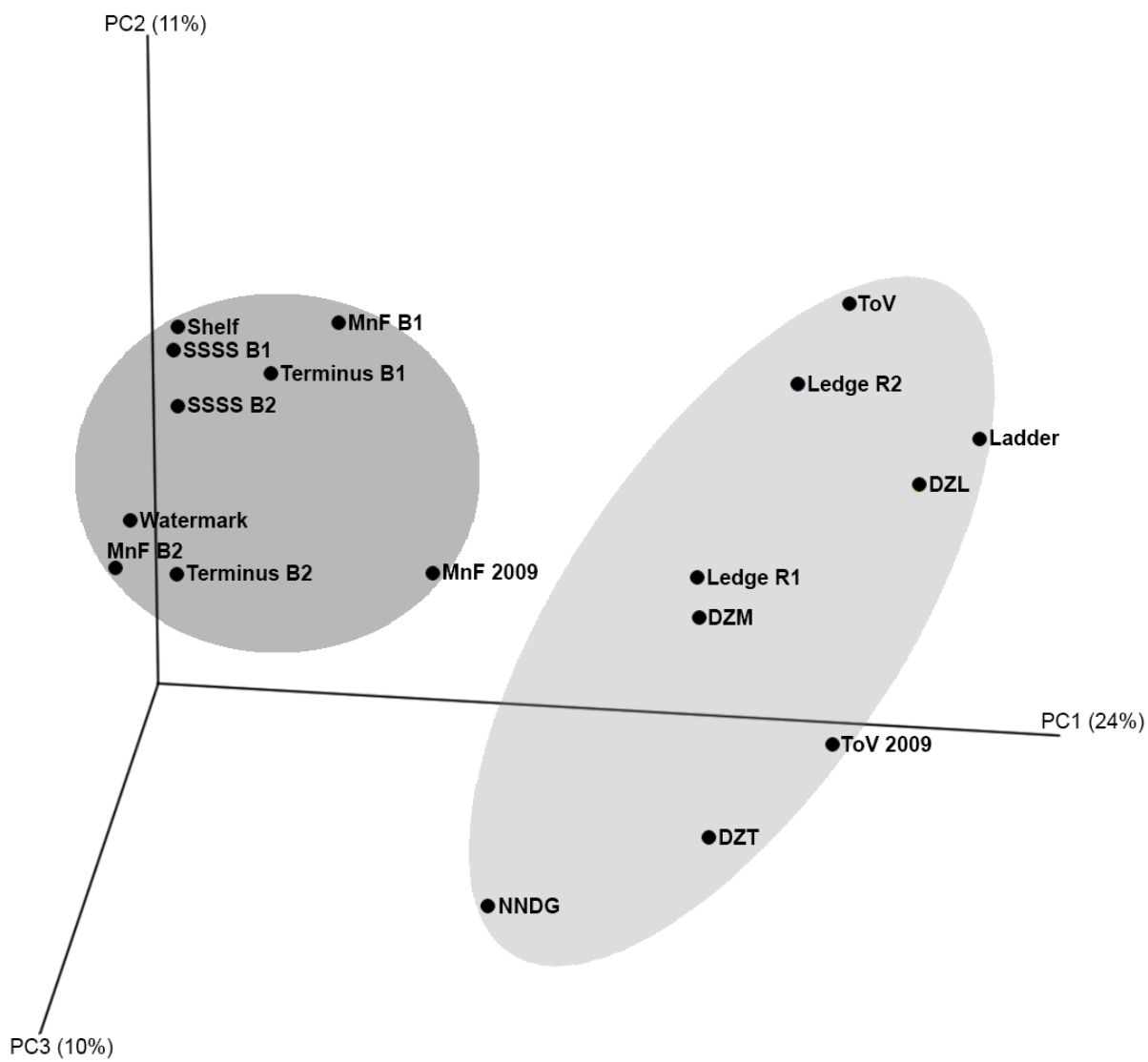
Figure 5. Principal coordinate analysis based on abundance-weighted Jaccard matrix of microbial communities sampled from either CSPC sediments (dark shade) or DBC sediments (light shade).

Nucleotide amplicon data indicated the proportion of sequences associated with OTUs at the phylum level within each cave was similar for Zygomycota spp. (CSPC: 5.74% ±1.54%, DBC: 3.58% ±0.97%) and unidentified fungi (CSPC: 13.11% ±2.40%, DBC: 11.34% ±4.24%), but differed significantly between Ascomycota spp. ($P = 0.0021$) and

Basidiomycota spp. ($P = 0.0026$) (Fig. 6). Within CSPC, OTU sequences identified as

Ascomycota spp. dominated at 57.94% ±5.24% followed by Basidiomycota spp. at 22.67%

±4.95%. Conversely, OTU sequences relating to Basidiomycota spp. within DBC dominated

at 47.51% ± 5.94% while Ascomycota spp. comprised 37.58% ±3.54% of the total fungal

taxa.
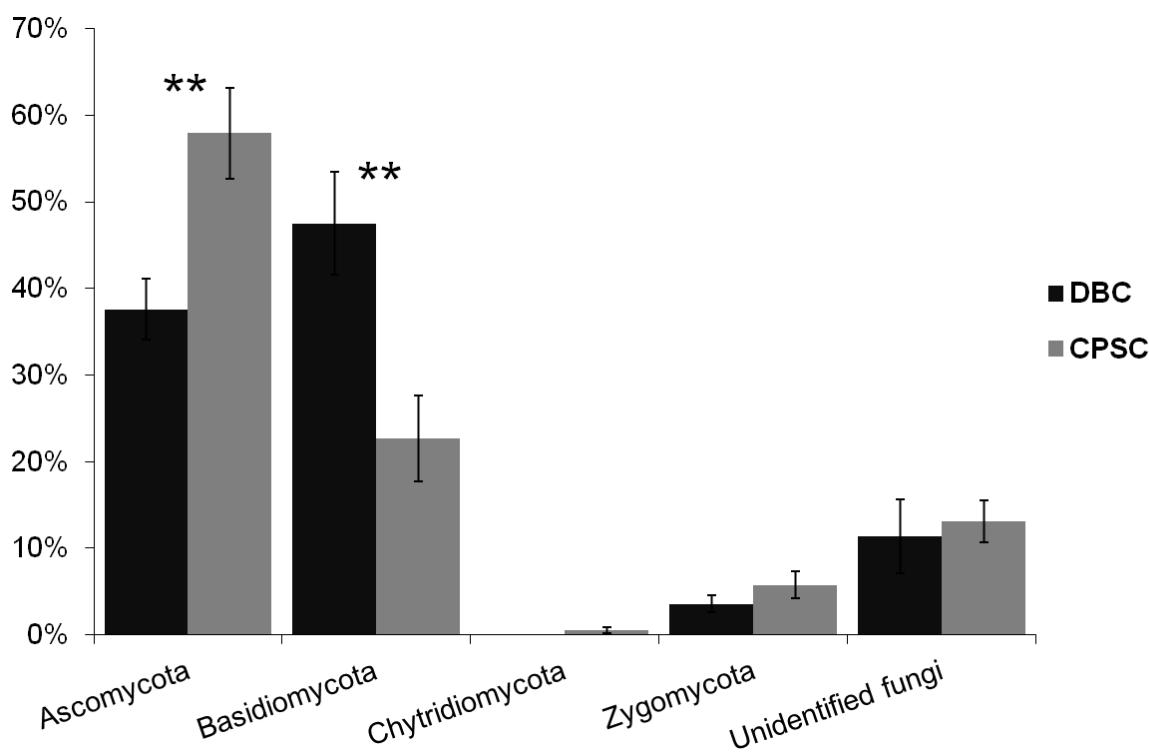
Figure 6. Averaged phylum-level distribution of sequences from DBC and CSPC baseline communities. Error bars represent standard error and double asterisks denote statistically significant ($P < 0.05$) differences according to a T-TEST.

Within DBC, OTU assignments within sample sites varied, with Ascomycetes

ranging from 26.40% to 56.50%, Basidiomycetes ranging from 24.40% to 65.80%,

Zygomycetes ranging from 0.10% to 8.70%, and unidentified fungi ranging from 1.30% to

37.30% of sequences (Fig. 7). In CSPC, however, OTUs were assigned at a range of 43.10% to 86.30% for Ascomycetes, Basidiomycetes ranging from 1.40% to 49.40%, Zygomycetes ranging from 0.90% to 9.30%, unidentified fungi ranging from 1.20% to 16.80%, in addition to Chytridiomycota species being recovered from Shelf and SSSS, ranging from 0.80% to 3.10% of sequences (Fig. 8).
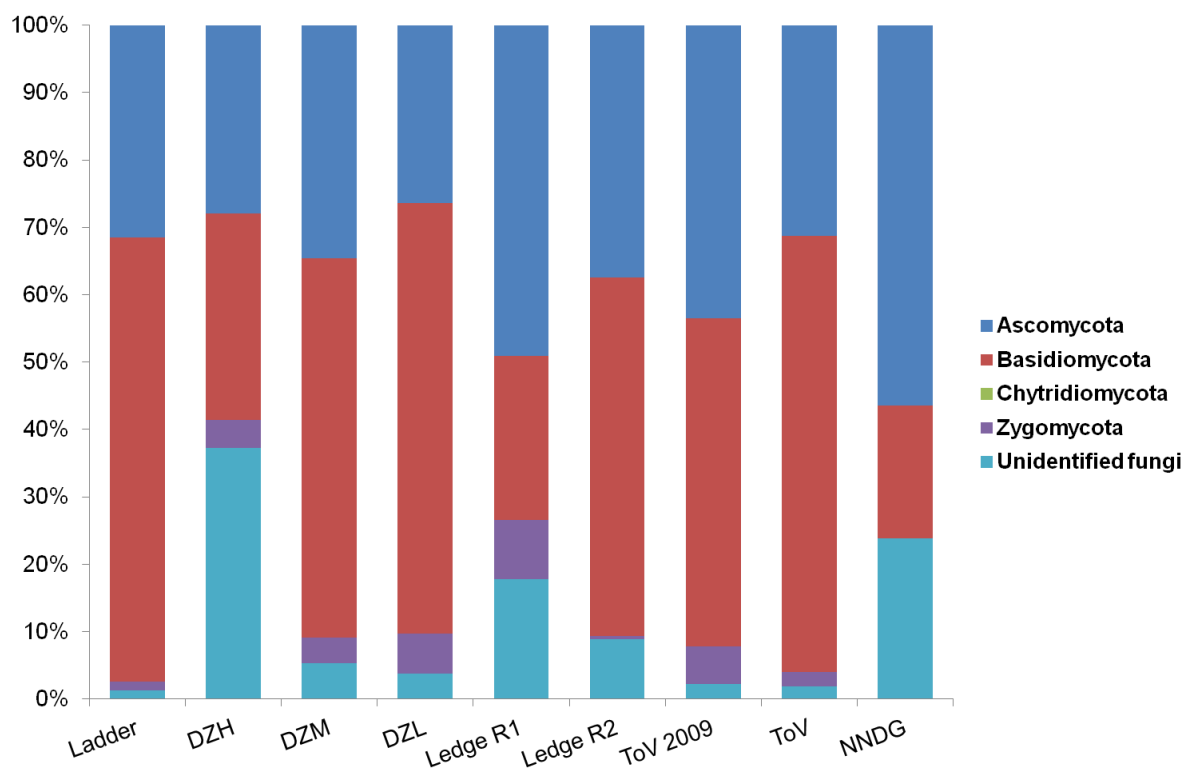
Figure 7. Phylum-level distribution of sequences within DBC.
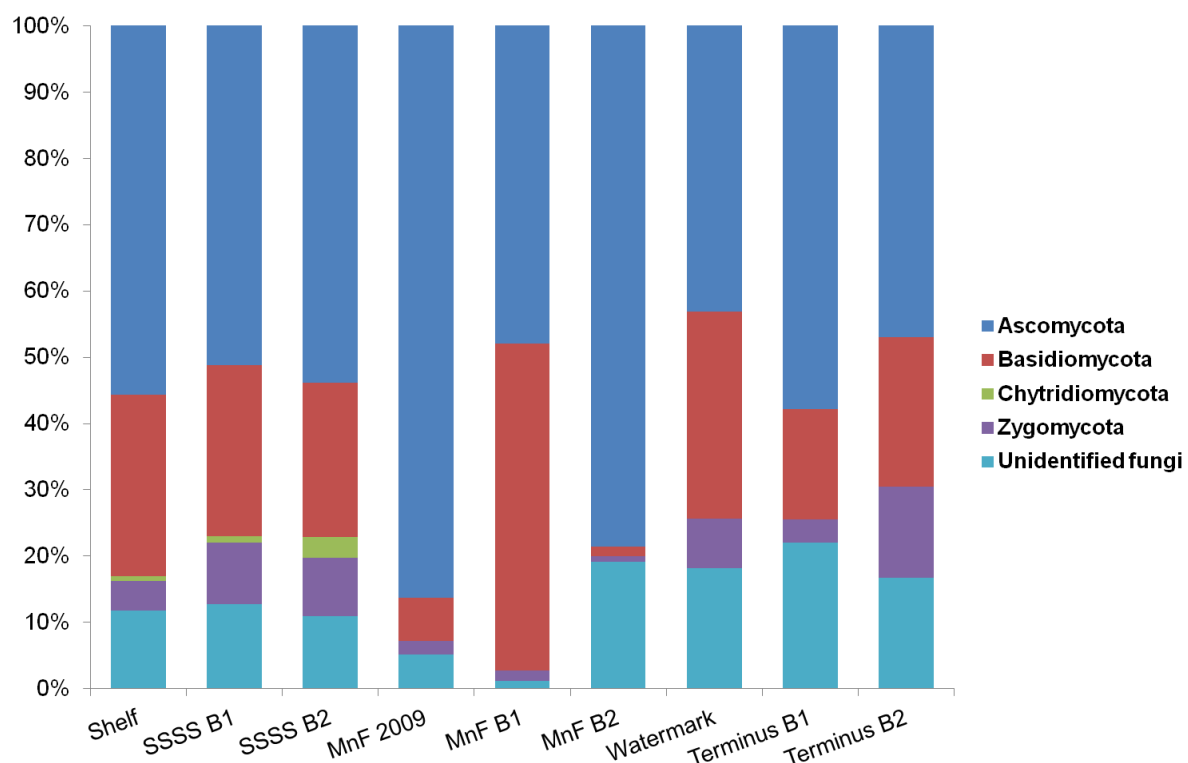
Figure 8. Phylum-level distribution of sequences within CSPC.

After sorting by total sequence count across all 9 sites within each cave, the top seven OTUs for DBC and CSPC were compared. Notably, the top 7 OTUs within CSPC reflected approximately 30% of total sequences attained for all samples within CSPC, while the top 7 OTUs within DBC reflected approximately 83%, suggesting greater species evenness among CSPC than DBC (Fig. 9). Surprisingly, only *Pseudogymnoascus verrucosus* was shared between cave sites.

A Carter Saltpeter Cave

Shelf	SSSS B1	SSSS B2	MnF 2009	MnF B1	MnF B2	Watermark	Terminus B1	Terminus B2	
2.4%	1.1%	1.5%	0.0%	0.0%	0.0%	0.2%	0.1%	0.1%	Ascomycota sp. AR 2010
0.1%	0.1%	0.1%	0.0%	0.0%	0.2%	0.1%	0.1%	4.4%	*Pseudogymnoascus verrucosus*
0.3%	0.3%	0.1%	0.0%	0.0%	0.0%	0.1%	2.6%	1.3%	Unidentified fungus (JN889968.1)
0.2%	0.1%	0.1%	0.0%	0.0%	0.0%	0.3%	1.7%	2.3%	*Rhizopogon pseudoroseolus*
1.5%	0.2%	1.1%	0.0%	0.5%	0.2%	0.2%	0.0%	0.5%	Uncultured tremellomycete (JX675151.1)
0.0%	0.0%	0.0%	0.0%	0.0%	2.9%	0.3%	0.0%	0.7%	Uncultured soil fungus (JF32996.1)
0.4%	0.6%	0.8%	0.0%	0.0%	0.1%	0.2%	0.4%	1.3%	*Mortierella* sp. CM1 45

B Daniel Boone Caverns

Ladder	DZL	DZM	DZH	Ledge R1	Ledge R2	ToV 2009	ToV	NNDG	
16.0%	3.4%	0.0%	0.1%	1.3%	14.6%	6.3%	0.1%	0.0%	*Coprinellus micaceus*
2.6%	0.9%	0.0%	0.1%	1.1%	6.2%	4.7%	0.1%	0.0%	*Pseudogymnoascus verrucosus*
3.3%	0.2%	0.0%	0.0%	0.2%	0.1%	0.0%	0.0%	0.7%	*Mollisia dextrinospora*
0.0%	0.0%	0.0%	0.0%	0.0%	0.0%	0.0%	0.0%	4.0%	*Aspergillus* sp. DY115 217 M6
0.6%	0.1%	0.0%	0.0%	0.1%	1.4%	0.7%	0.0%	0.7%	*Onygenales* sp. 7R17 3
0.3%	0.1%	0.0%	0.0%	0.9%	2.0%	0.0%	0.0%	0.0%	Uncultured fungus (JX975978.1)
0.1%	0.0%	0.0%	0.0%	0.0%	2.6%	0.0%	0.0%	0.0%	*Ganoderma applanatum*

Figure 9. Heatmap of the percentage of sequences represented from each of the top OTUs within (A) CSPC and (B) DBC, respectively. Highest ranking accession number from BLAST search is represented within parenthesis for unidentified and uncultured OTUs.

Most of the families reported across other cave studies (see review by Vanderwolf,

Malloch, McAlpine, and Forbes, 2013) were also detected here (Table 3).

Table 3. Relative percentages of top fungi reported in caves. The abundances of the most frequently isolated fungi, adapted from Vanderwolf et al. (2013), were calculated as a percentage of the 1,813 isolates reported from the review (excluding the slime mold group Dictyosteliaceae). Also shown are the corresponding Illumina-based percentages found within the CSPC and DBC cave systems studied here.

Family	Abundances as reviewed by Vanderwolf et al.	Illumina-based estimates of abundances in CSPC and DBC
Trichocomaceae	34.197%	7.529%
Mucoraceae	8.163%	0.029%
Nectriaceae	5.847%	0.027%
Laboulbeniaceae	5.792%	0.000%
Pleosporaceae	4.744%	0.409%
Microascaceae	4.247%	0.004%
Hypocreaceae	4.247%	0.013%
Cordycipitaceae	4.192%	0.000%
Chaetomiaceae	3.971%	0.118%
Bionectriaceae	3.861%	0.009%
Davidiellaceae	3.530%	0.011%
Myxotrichaceae	2.758%	1.161%
Polyporaceae	2.758%	0.041%
Arthrodermataceae	2.648%	0.038%
Mortierellaceae	2.427%	5.213%
Clavicipitaceae	1.820%	0.006%
Fomitopsidaceae	1.655%	0.030%
Psathyrellaceae	1.600%	11.794%
Mycenaceae	1.544%	0.000%

Enriched versus baseline communities

In the three sites that showed Mn(II) oxidation, a net increase in bacterial abundance

was observed. Bacterial SSU rRNA genes demonstrated an increase of cells per gram wet

weight from an average of 2.83×10^9 to $7.46 \ 6.37 \times 10^9$ for site SSSS, 8.25×10^8 to $1.54 \times$

10^9 for MnF, and $9.72.83 \times 10^8$ to 6.66×10^9 for Terminus (Fig. 10). Fungal consortia

changed more dramatically among two sites, with an increase of cells per gram wet weight from an average of 9.63 x 10^4 to 8.48 x 10^7 for site SSSS and 7.13 x 10^4 to 8.29 x 10^5 for Terminus. A net reduction in fungal cells per gram wet weight was observed at the MnF site with decrease from the basal average of 2.06 x 10^5 to 1.22 x 10^5 cells per gram wet weight.
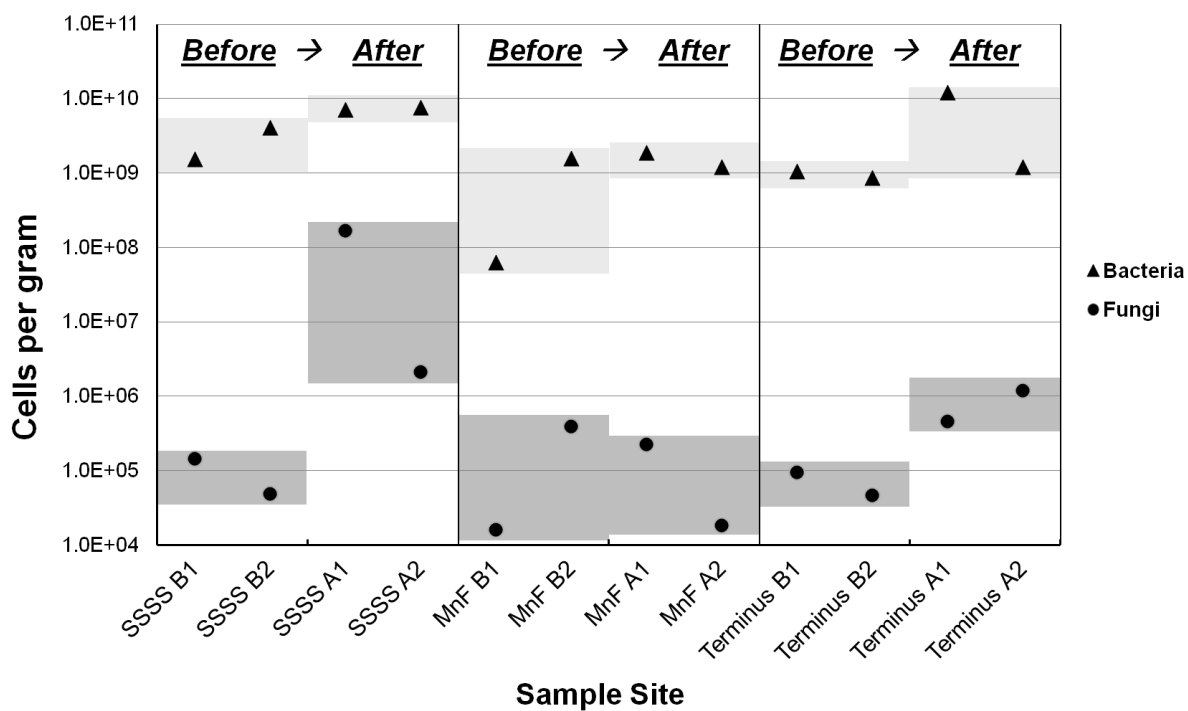

Figure 10. Estimated number of bacterial (red) and fungal (blue) cells per gram wet weight before (B1, B2) and after (A1, A2) *in-situ* Mn oxidation was observed. Cell abundance was estimated from real-time qPCR quantification of the SSU rRNA gene for bacteria or the ITS region for fungi.

A strong shift in taxonomic distribution was observed among OTUs after enrichment with significant decreases in Ascomycota (56.07% ±4.77% to 27.50% ±10.68, $p = 0.022$) and Basidiomycota (23.17% ±6.35% to 2.82% ±1.18, $p = 0.011$), but also a significant increase of Zygomycota (6.30% ±2.09% to 37.72% ±12.42, $p = 0.031$) (Fig. 11).
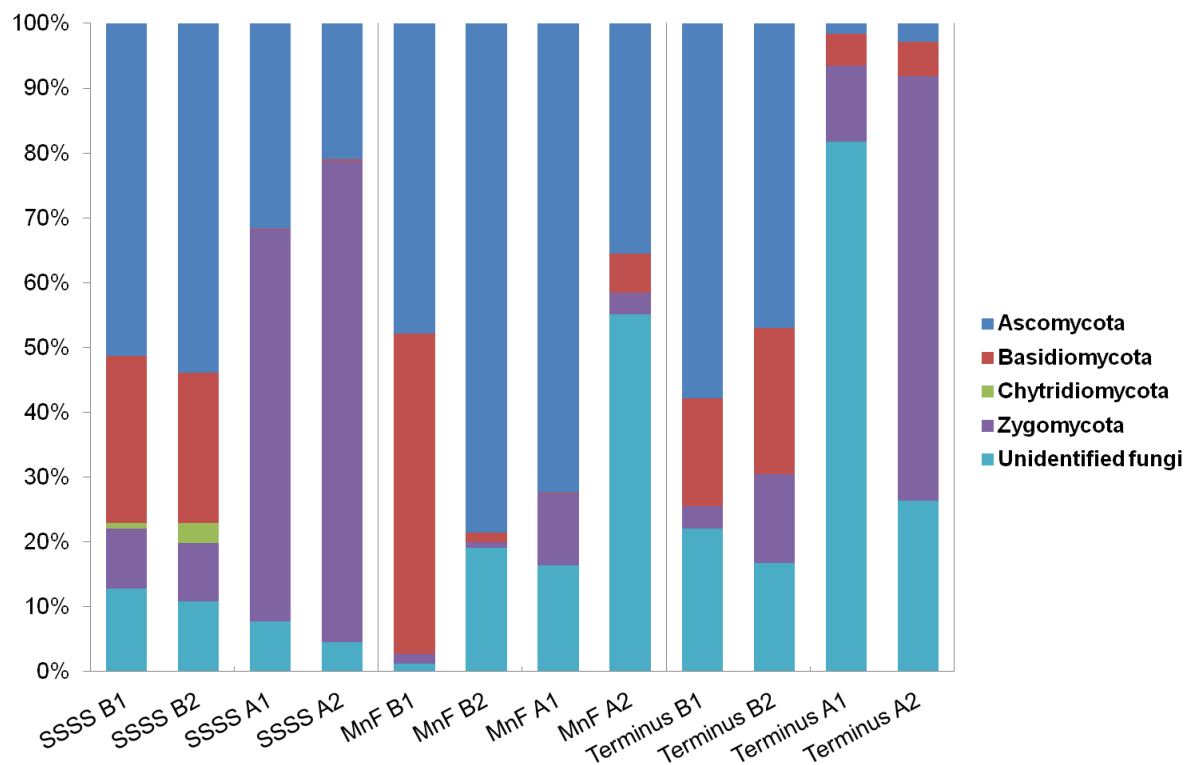
Figure 11. Phylum-level distribution of sequences within CSPC sample sites before (B1, B2) and after (A1, A2) *in-situ* Mn oxidation was observed.

The phylogenetic shift of fungal assemblages observed after enrichment compared to before enrichment showed changes a shift towards most notably, *Mortierella* spp-related sequences, which only accounted for 1.9% of sequences within CSPC before nutrient loading, to representing the majority (35.0%) of sequences across all sites after enrichment (Table 4). Alpha diversity estimates demonstrated a significant ($P < 0.05$) decrease in values across all metrics for the SSSS site, or for only the Shannon and Simpson values across all sites (Table 5). The overall net decrease in richness/diversity indices suggests a shift toward a less diverse community. In addition, PCoA using Bray-Curtis beta diversity shows the trend of dissimilarity between before and after communities in all dimensions for each site (Fig. 12).

Table 4. Relative abundance of the top three OTUs from respective sites before and after enrichment.

Site name and top OTUs	Relative abundance	Site name and top OTUs	Relative abundance
SSSS Before		**SSSS After**	
Pholiota burkei	1.79%	*Mortierella biramosa*	7.12%
Trichosporon moniliiforme	1.74%	*Epicoccum nigrum*	0.21%
Pseudogymnoascus verrucosus	0.59%	*Cladophialophora chaetospira*	0.20%
MnF Before		**MnF After**	
Oidiodendron maius	4.23%	*Mortierella* sp.	6.40%
Amanita bisporigera	3.76%	*Penicillium polonicum*	5.04%
Umbelopsis dimorpha	3.42%	*Jahnula aquatica*	4.79%
Terminus Before		**Terminus After**	
Pseudogymnoascus verrucosus	5.56%	*Mortierella biramosa*	7.76%
Rhizopogon pseudoroseolus	5.00%	*Trichosporon wieringae*	1.36%
Jahnula aquatica	1.89%	*Pseudogymnoascus verrucosus*	0.22%

Table 5. Alpha diversity estimates before (B1, B2) and after (A1, A2) nutrient loading using ACE, Chao1, Simpson, Shannon, and Observed Species metrics. Average values across all three sites are shown for data collected both before and after enrichment. P-value results from a T-TEST comparing the before and after samples is shown for each metric. A significant P values is denoted by an asterisk (*).

|	ACE	Chao1	Simpson	Shannon	Observed Species
SSSS B1	524.04	521.28	0.97	6.54	482
SSSS B2	520.65	525.93	0.96	5.87	456
MnF B1	54.74	49	0.7	2.57	44
MnF B2	145.03	130.25	0.84	3.13	107
Terminus B1	205.46	203.25	0.94	5.02	186
Terminus B2	302.5	278.44	0.93	5.2	244
Average Before	292.07	284.692	0.89	4.72167	253.167
SSSS A1	244.55	245.33	0.75	2.53	173
SSSS A2	202.82	214	0.64	2.22	136
MnF A1	126.7	109.5	0.83	2.91	90
MnF A2	210	214.55	0.71	3.21	140
Terminus A1	151.13	152.23	0.65	2.18	101
Terminus A2	142.57	147.33	0.77	2.79	106
Average After	179.628	180.49	0.725	2.64	124.333
P-value	*0.11183*	*0.13283*	***0.00561***	***0.01041****	*0.07126*
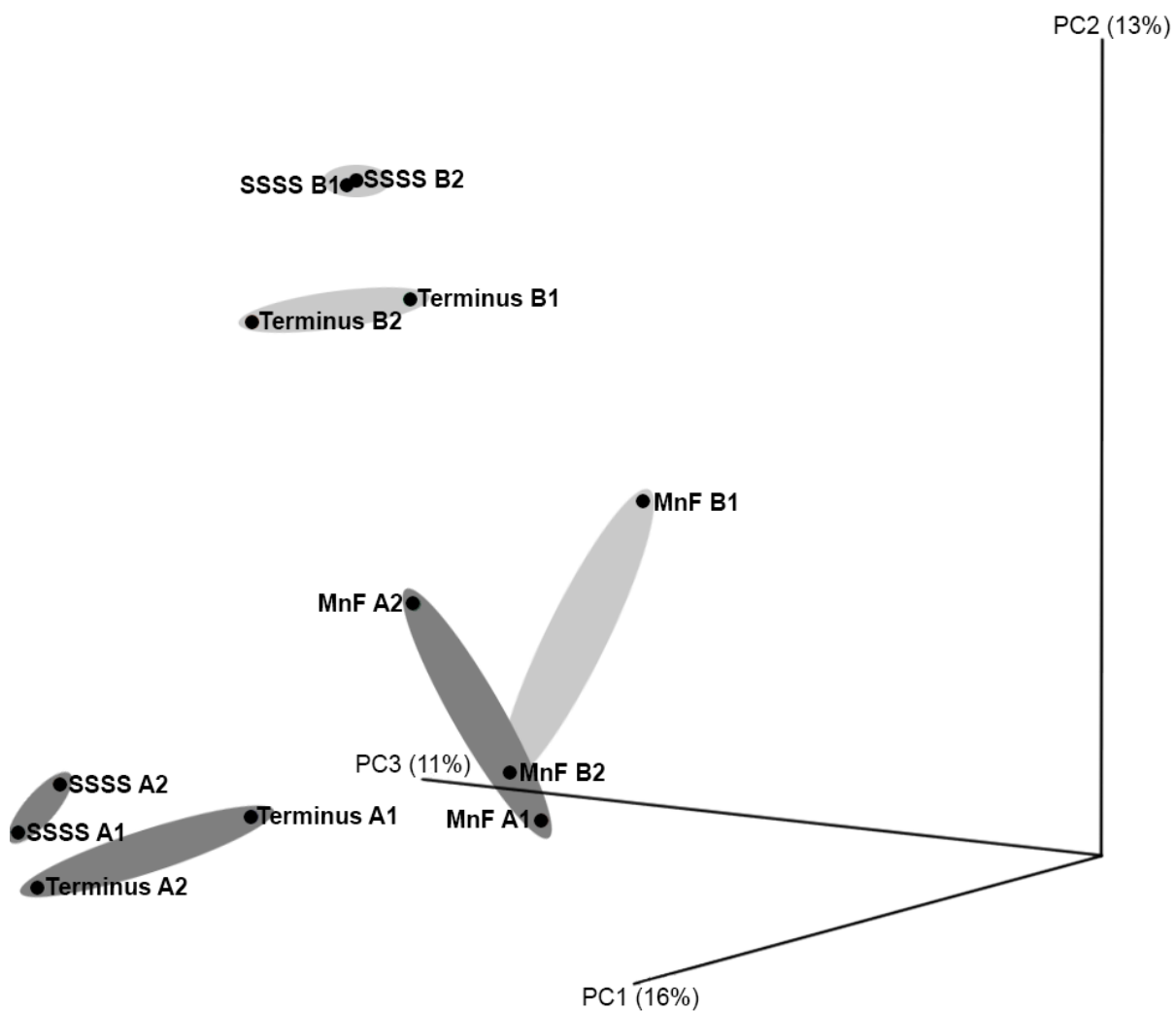
Figure 12. Bray-Curtis PCoA before and after *in-situ* Mn oxidation. PCoA matrices of microbial communities sampled from CSPC sediments either before (light shades) incubation with exogenous carbon and stimulation of Mn(II) oxidation or after (dark shades).

DISCUSSION

Sequencing

The choice of primers for the fungal ITS1 gene can greatly influence the phylogenetic distribution of sequences amplified during PCR reactions (Anderson et al., 2009). Thus, triplicate reactions were amplified and pooled for each sample in order to reduce bias. Further, a touchdown PCR protocol was used to help prevent primer dimer formation (Bräuer et al., 2014) and to further minimize primer bias (Korbie & Mattick, 2008). Even so, many OTUs chosen at a 99% identity *denovo* returned as "No Blast Hit" when matched against UNITE. Manual BLAST searches of these sequences resulted with hits relating to protozoans, undefined fungal amplicons, and other organisms. It is also important to note that grouping OTUs at 99% sequence identity cutoff resulted in OTU table sizes up to two orders of magnitude larger than those produced from a 97% sequence similarity. Thus, because the 99% OTU table size exponentially increased CPU working time, these analyses were precluded. For this reason, a closed reference OTU picking strategy at 97% sequence similarity was employed in order to return the most computationally efficient, phylogenetically relevant, and taxonomically confident sequence assignments.

Baseline cave communities

Cell Counts

The conservative approximation of 150 ITS1 rRNA copies per fungal cell during qPCR standardization may have led to an underestimation of fungal cell abundance as the quantity of rDNA genes per cell can vary widely across fungal phyla (Herrera, Vallor, Gelfond, Patterson, & Wickes, 2009; Longo et al., 2013). Further, it is important to note that the estimated cell counts may or may not be representative of biomass, but does provide a method of comparison across various sites and samples. In contrast, a more precise copy number could be determined for bacterial 16S rRNA using the Ribosomal RNA Operon Copy Number Database (Klappenbach, Saxman, Cole, & Schmidt, 2001). This normalization led to the approximation of $1.0x10^4$ bacterial cells per fungal cell within CSPC, and $1.2x10^4$ bacterial cells per fungal cell within DBC. Overall, the data indicate that while the impacted cave yielded on average an order of magnitude greater number of cells per gram of bacteria and fungi, the proportion of fungi compared to bacteria within each cave remained similar. In other words, bacterial and fungal cells were enriched to a similar degree. The average ratio of fungi:bacteria based on gene copy number per nanogram was 0.007 ($\sigma = 0.069$) for CSPC samples, and 0.004 ($\sigma = 0.027$) for DBC. While there was no statistical difference between the number of fungal ITS1 copies, there was a significant difference for SSU bacterial gene copies between caves ($P = 0.027$). On the other hand, when copy numbers were normalized to estimate cell counts per gram of soil, significant differences between each cave were found for both bacteria ($P = 0.007$) and fungi ($P = 0.012$). Other studies have analyzed topsoil communities and found that the ratio of fungi:bacteria in terms of ITS1 and 16S copy numbers varies within cultivated, pasture, hardwood, and pine-stand soil communities from

0.0216 to 0.1018 (Lauber et al., 2008), but can reach 1 or higher in some cases such as mycorrhizal rhizospheres rich in carbon (Baldrian et al., 2012; Fierer et al., 2005). In our study, the overall ratio across all 18 samples was extremely low (0.021, $\sigma = 0.051$) compared to topsoil, which may be attributed to lower nutrient availability (Carmichael et al., 2013b), dearth of symbionts, or a lack of leaf litter (Baldrian et al., 2012).

Community composition and diversity

Two groups not detected in our study that were most frequently cultured from the Vanderwolf et al. (2013) review were Laboulbeniaceae and Cordycipitaceae, both of which contain entomoparasitic members (Table 4). Similarly, OTUs within the entomopathic order of Hypocreales (specifically the family Clavicipitaceae) were found only within CSPC in relatively-low abundance (0.006%). These differences in sequences abundances may be at least partially explained by the prevalence of culture-based techniques among the studies reviewed by Vanderwolf et al. (2013) which may be less representative of the true abundances compared to the molecular techniques employed here. Another notable difference is the lack of sequences from the family Mycenaceae, a globally widespread and ecologically diverse family of fungi (Alves & Nascimento, 2014; Li, Zhu, Liu, & Zhu, 2012). As some species from this family could be considered an invasive species (Vizzini, Zotti, & Mello, 2009), the deficit of representatives may reflect the more isolated ecology of the caves studied here compared to show caves in Europe that commonly receive hundreds of thousands of visitors per year (Bastian et al., 2010).

The dominant families within DBC were represented by sequences within the Psathyrellaceae and Pseudeurotiaceae, namely *Coprinellus micaceus* (41.9%) and

Pseudogymnoascus verrucosus (17.0%), respectively. *Coprinellus micaceus*, formerly classified within the genus *Coprinus* is a saprophytic fungus responsible for late phase decomposition (Peiris et al., 2008), likely reflecting the highly limited nutrient input as expected for a near-pristine cave. Within CSPC, OTUs were much more evenly distributed and demonstrated greater species richness, with dominant OTUs assigned to Pseudeurotiaceae (7.2%), Trichocomaceae (9.5%), Incertae sedis Helotiales (11.0%), Orbiliaceae (0.2%), unknown Tremellales (4.4%), and ectomycorrhizal Rhizopogonaceae spp. (5.6%). A unique characteristic of CSPC when compared to DBC is the incidence of Chytridiomycota species *Spizellomyces acuminatus* and *Powellomyces* sp. EA. Although comprising only 0.7% of sequences from three samples associated with CSPC, these Chytridiomycota-related sequences may be a product of greater hydrologic input in CSPC (Carmichael et al., 2013b). Interestingly, one dominant OTU that was found in both caves, *Pseudogymnoascus verrucosus,* is related to the causative agent of white nose syndrome, *Pseudogymnoascus destructans* (Minnis & Lindner, 2013). Further, members of this genus have been cultured from caves and show saprotrophic growth properties (Reynolds & Barton, 2014).

Mn oxide enrichment community cell counts and phylogenetic shifts

Among the three sites observed to have a noticeable increase in Mn(II)-oxidation none had significant changes in bacterial or fungal numbers when comparing the before samples to those collected after stimulation. Ratios of fungal:bacterial gene copy numbers increased greatly after enrichment for SSSS (0.002 to 0.513) but only slightly for Terminus (0.003 to 0.007). After exposure to glucose casts, a strong increase in cell numbers of

bacteria and fungi was observed in samples from SSSS and Terminus, whereas estimated fungal cell quantity dropped slightly at the MnF site. Additionally, a proportional decrease in fungal:bacterial gene copy ratio (from 0.009 to 0.004) was observed. This was an expected finding, as MnF was found to contain blooms of bacteria that produced biogenic Mn oxides as a result of exogenous carbon input (Carmichael et al., 2013a).

Notably, *Mortierella* spp. were consistently enriched by glucose additions in the field. However, the estimates of *Mortierella* spp. abundance in samples may be proportionally low as some OTUs may not have been properly identified. As an example, at least one OTU from DBC (2,085 associated sequences) identified as an uncultured fungus, but when subject to a BLAST search, revealed 100% identity with several *Mortierella* spp. strains including: *Mortierella elongata* (JX975978.1, HQ630362.1), *Mortierella* sp. NCP 07/05 (JX243796.1), 02/08 (JX243792.1), 02/06 (JX243791.1), and *Mortierella* sp. 68 (EU877759.1) among others. Including this "uncultured fungus" OTU into proportional estimates of *Mortierella* spp. found within DBC would shift the perceived presence from 2.3% to approximately 5.5%. One Mn(II)-oxidizing enrichment culture from sediment within CSPC, "Black Dots," was found to be dominated by an organism that grouped closely with other cultured *Mortierella* spp. strains, and shared 97% identity to *Mortierella dichotoma* strains 68 and CB (Cara Santelli, unpublished data). *Mortierella*'s ecology is globally widespread and could be described as a constituent saprobe of the general soil microbiome (Cabello & Arambarri, 2002; Orgiazzi et al., 2013). Members of this species prefer simple carbon substrates such as glucose (Higashiyama, Fujikawa, Park, & Shimizu, 2002), and at least one *Mortierella* spp. strain (black dots) is shown here to also be a prominent primary colonizer of solid forms of simple carbon sources within cave environments as well.

CONCLUSIONS

Between these two caves systems, ferromanganese oxide deposits were found to differ significantly in both abundance and community structure of fungal cells harbored therein. Within the near-pristine environment of DBC, sediment samples produced lower estimates of species evenness, richness, diversity, and even sequences present. In contrast, the anthropogenically impacted cave studied here had significantly greater numbers of cells within the baseline community, higher alpha diversity estimates, as well as notably different phylogenetic assemblages. In a previous study (Carmichael et al., 2013a), bacterial Mn(II) oxidation was strongly correlated with liquid exogenous carbon input. Here, we show that solid exogenous carbon sources can lead to increased production of Mn oxides associated with the enrichment of common soil fungi and dramatic changes in fungal population dynamics. This research demonstrates that microbial communities respond to carbon input in dynamic ways, sometimes resulting in Mn oxide deposition. Further, results suggest that Mn(II) oxidation is a carbon-driven process in these epigenic cave systems.

REFERENCES

Abarenkov, K., Nilsson, R. H., Larsson, K. H., Alexander, I. J., Ebenhardt, U., Erland, S., . . . Koljalg, U. (2010). The UNITE database for molecular identification of fungi - recent updates and future perspectives. *New Phytologist, 186*(2), 1447-1452.

Aguirre, J., Rios-Momberg, M., Hewitt, D., & Hansberg, W. (2005). Reactive oxygen species and development in microbial eukaryotes. *Trends in Microbiology, 13*(3), 111-118. doi: DOI 10.1016/j.tim.2005.01.007

Altschul, S. F., Gish, W., Miller, W., Myers, E. W., & Lipman, D. J. (1990). Basic local alignment search tool. *Journal of Molecular Biology, 215*(3), 403-410.

Alves, M. H., & Nascimento, C. (2014). *Mycena margarita* (Murrill) Murrill, 1916 (Basidiomycota: Agaricales: Mycenaceae): A bioluminescent agaric first recorded in Brazil. *Check List, 10*(1), 239-243.

Anderson, I. C., & Cairney, J. W. G. (2004). Diversity and ecology of soil fungal communities: increased understanding through the application of molecular techniques. *Environmental Microbiology, 6*(8), 769-779. doi: DOI 10.1111/j.1462-2920.2004.00675.x

Anderson, C. R., Johnson, H. A., Caputo, N., Davis, R. E., Torpey, J. W., & Tebo, B. M. (2009). Mn(II) oxidation is catalyzed by heme peroxidases in "*Aurantimonas manganoxydans*" strain SI85-9A1 and *Erythrobacter* sp. strain SD-21. *Applied and Environmental Microbiology, 75*(12), 4130-4138.

Baldrian, P., Kolarik, M., Stursova, M., Kopecky, J., Valaskova, V., Vetrovsky, T., . . . Voriskova, J. (2012). Active and total microbial communities in forest soil are largely different and highly stratified during decomposition. *ISME J, 6*, 248-258.

Bastian, F., Jurado, V., Novakova, A., Albouvette, C., & Saiz-Jimenez, C. (2010). The microbiology of Lascaux cave. *Microbiology, 156*, 644-652.

Bedard, K., & Krause, K. H. (2007). The NOX family of ROS-generating NADPH oxidases: physiology and pathophysiology. *Physiological Reviews, 87*(1), 245-313. doi: DOI 10.1152/physrev.00044.2005

Bodei, S., Manceau, A., Geoffroy, N., Baronnet, A., & Buatier, M. (2007). Formation of todorokite from vernadite in Ni-rich hemipelagic sediments. *Geochimica Et Cosmochimica Acta, 71*(23), 5698-5716. doi: DOI 10.1016/j.gca.2007.07.020

Braud, A., Hoegy, F., Jezequel, K., Lebeau, T., & Schalk, I. J. (2009). New insights into the metal specificity of the *Pseudomonas aeruginosa* pyoverdine-iron uptake pathway. *Environmental Microbiology, 11*(5), 1079-1091. doi: DOI 10.1111/j.1462-2920.2008.01838.x

Bräuer, S. L., Adams, C., Kranzler, K., Murphy, D., Xu, M., Zuber, P., . . . Tebo, B. M. (2011). Culturable *Rhodobacter* and *Shewanella* species are abundant in estuarine turbidity maxima of the Columbia River. *Environmental Microbiology, 13*(3), 589-603.

Bräuer, S. L., Vuono, D., Carmichael, M. J., Pepe-Ranney, C., Strom, A., Rabinowitz, E., . . . Zinder, S. (2014). Microbial sequencing analyses suggest the presence of a fecal veneer on indoor climbing wall holds. *Current Microbiology, Accepted*.

Buee, M., Reich, M., Murat, C., Morin, E., Nilsson, R. H., Uroz, S., & Martin, F. (2009). 454
Pyrosequencing analyses of forest soils reveal an unexpectedly high fungal diversity.
New Phytologist, 184(2), 449-456. doi: DOI 10.1111/j.1469-8137.2009.03003.x

Burns, R. G., Burns, V. M., & Stockman, H. W. (1983). A review of the todorokite buserite
problem - implications to the mineralogy of marine manganese nodules. *American
Mineralogist, 68*(9-10), 972-980.

Cabello, M., & Arambarri, A. (2002). Diversity in soil fungi from undisturbed and disturbed
Celtis tala and *Scutia buxifolia* forests in the eastern Buenos Aires province
(Argentina). *Microbiological Research, 157*, 115-125.

Caporaso, J. G., Kuczynski, J., Stombaugh, J., Bittinger, K., Bushman, F. D., Costello, E. K.,
. . . Knight, R. (2011). QIIME allows analysis of high-throughput community
sequencing data. *Nature Methods, 7*(5), 335-336.

Caporaso, J. G., Lauber, C. L., Walters, W. A., Berg-Lyons, D., Huntley, J., Fierer, N., . . .
Knight, R. (2012). Ultra-high-throughput microbial community analysis on the
Illumina HiSeq and MiSeq platforms. *Isme Journal, 6*(8), 1621-1624. doi: Doi
10.1038/Ismej.2012.8

Carmichael, M. J., Carmichael, S. K., Santelli, C. M., Strom, A., & Bräuer, S. L. (2013a).
Mn(II)-oxidizing bacteria are abundant and environmentally relevant members of
ferromanganese deposits in caves of the upper Tennessee river basin.
Geomicrobiology Journal, 30(9), 779-800. doi: Doi 10.1080/01490451.2013.769651

Carmichael, S. K., & Bräuer, S. L. (In review). Microbial diversity of manganese cycling in
cave and karst settings. In K. J. & D. Wagner (Eds.), *Microbial Life of Cave Systems*.
Boston, MA: Walter de Gruyter, Inc.

Carmichael, S. K., Carmichael, M. J., Strom, A., Johnson, K. W., Roble, L. A., Gao, Y., & Bräuer, S. L. (2013b). Sustained anthropogenic impact in Carter Saltpeter Cave, Carter County, Tennessee and the potential effects on manganese cycling. *Journal of Cave and Karst Studies*, 1-16. doi: 10.4311/2012mb0267

Corstjens, P. L. A. M., de Vrind, J. P. M., Goosen, T., & de Vrind-de Jong, E. W. (1997). Identification and molecular analysis of the *Leptothrix discophora* SS-1 mofA gene, a gene putatively encoding a manganese-oxidizing protein with copper domains. *Geomicrobiology Journal, 14*(2), 91-108.

Cunningham, K. I., Northup, D. E., Pollastro, R. M., Wright, W. G., & LaRock, E. J. (1995). Bacteria, Fungi, and Biokarst in Lechuguilla Cave, Carlsbad Caverns National Park, New Mexico. *Enironmental Geology, 25*, 2-8.

Davis, R. E., & Tebo, B. M. (2013). *Culture-independent identification of manganese oxidizing genes from deep-sea hydrothermal vent chemoautotrophic ferromanganese microbial communities using a metagenomic approach.* Paper presented at the American Geophysical Union: Fall Meeting, San Francisco, CA.

Delatorre, M. A., & Gomezalarcon, G. (1994). Manganese and iron oxidation by fungi isolated from building stone. *Microbial Ecology, 27*(2), 177-188.

Downs, R. (2006). *The rruff project: an integrated study of the chemistry, crystallography, raman and infrared spectroscopy of minerals.* Paper presented at the General Meeting of the International Mineralogical Association, Kobe, Japan.

Duckworth, O. W., Bargar, J. R., & Sposito, G. (2008). Sorption of ferric iron from ferrioxamine b to synthetic and biogenic layer type manganese oxides. *Geochimica Et Cosmochimica Acta, 72*(14), 3371-3380. doi: DOI 10.1016/j.gca.2008.04.026

Edgar, R. C., Haas, B. J., Clemente, J. C., Quince, C., & Knight, R. (2011). UCHIME improves sensitivity and speed of chimera detection. *Bioinformatics, 27*(16), 2194-2200.

Einen, J., Thorseth, I. H., & Ovreas, L. (2008). Enumeration of archaea and bacteria in seafloor basalt using real-time quantitative pcr and fluorescence microscopy. *Fems Microbiology Letters, 282*(2), 182-187. doi: DOI 10.1111/j.1574-6968.2008.01119.x

Feng, Q., Kanoh, H., & Ooi, K. (1999). Manganese oxide porous crystals. *Journal of Materials Chemistry, 9*(2), 319-333. doi: Doi 10.1039/A805369c

Fierer, N., Jackson, J. A., Vilgalys, R., & Jackson, R. B. (2005). Assessment of soil microbial community structure by use of taxon-specific quantitative PCR assays. *Applied Environmental Microbiology, 71*(7), 4117-4120. doi: 10.1128/AEM.71.7.4117-4120.2005

Fogel, G. B., Collins, C. R., Li, J., & Brunk, C. F. (1999). Prokaryotic genome size and SSU rDNA copy number: estimation of microbial relative abundance from a mixed population. *Microbial Ecology, 38*(2), 93-113. doi: DOI 10.1007/s002489900162

Gadd, G. M. (1999). Fungal production of citric and oxalic acid: importance in metal speciation, physiology and biogeochemical processes. *Advances in Microbial Physiology, 41*, 47-92. doi: Doi 10.1016/S0065-2911(08)60165-4

Gardes, M., & Bruns, T. D. (1993). ITS primers with enhanced specificity for basidiomycetes- application to the identification of mycorrhizae and rusts. *Molecular Ecology, 2*, 113-118.

Geszvain, K., Butterfield, C., Davis, R. E., Madison, A. S., Lee, S. W., Parker, D. L., . . . Tebo, B. M. (2012). The molecular biogeochemistry of manganese(II) oxidation. *Biochemical Society Transactions, 40*, 1244-1248. doi: Doi 10.1042/Bst20120229

Geszvain, K., McCarthy, J. K., & Tebo, B. M. (2013). Elimination of manganese(II/III) oxidation in *Pseudomonas putida* GB-1 by a double knockout of two putative multicopper oxidase genes. *Applied and Environmental Microbiology, 79*(1), 357-366. doi: Doi 10.1128/Aem.01850-12

Giesbert, S., Schurg, T., Scheele, S., & Tudzynski, P. (2008). The NADPH oxidase cpnox1 is required for full pathogenicity of the ergot fungus *Claviceps purpurea*. *Molecular Plant Pathology, 9*(3), 317-327. doi: Doi 10.1111/J.1364-3703.2008.00466.X

Grangeon, S., Lanson, B., Miyata, N., Tani, Y., & Manceau, A. (2010). Structure of nanocrystalline phyllomanganates produced by freshwater fungi. *American Mineralogist, 95*(11-12), 1608-1616. doi: Doi 10.2138/Am.2010.3516

Grote, G., & Krumbein, W. E. (1992). Microbial precipitation of manganese by bacteria and fungi from desert rock and rock varnish. *Geomicrobiology Journal, 10*(1), 49-57.

Hansel, C. M., Zeiner, C. A., Santelli, C. M., & Webb, S. M. (2012). Mn(II) oxidation by an ascomycete fungus is linked to superoxide production during asexual reproduction. *Proceedings of the National Academy of Sciences of the United States of America, 109*(31), 12621-12625. doi: DOI 10.1073/pnas.1203885109

Herrera, M. L., Vallor, A. C., Gelfond, J. A., Patterson, T. F., & Wickes, B. L. (2009). Strain-dependent variation in 18S ribosomal DNA copy numbers in *Aspergillus fumigatus*. *Journal of Clinical Microbiology, 47*(5), 1325-1332.

Heyworth, P. G., Bohl, B. P., Bokoch, G. M., & Curnutte, J. T. (1994). Rac translocates independently of the neutrophil nadph oxidase components p47(phox) and p67(phox) - evidence for its interaction with flavocytochrome b(558). *Journal of Biological Chemistry, 269*(49), 30749-30752.

Higashiyama, K., Fujikawa, S., Park, E. Y., & Shimizu, S. (2002). Production of arachidonic acid by *Mortierella* fungi. *Biotechnology and Bioprocess Engineering, 7*, 252-262.

Holzberg, M., & Artis, W. M. (1983). Hydroxamate siderophore production by opportunistic and systemic fungal pathogens. *Infection and Immunity, 40*(3), 1134-1139.

Johnson, K. W., Carmichael, M. J., McDonald, W., Rose, N., Pitchford, J., Windelspecht, M., . . . Brauer, S. L. (2012). Increased abundance of *Gallionella* spp., *Leptothrix* spp. and total bacteria in response to enhanced Mn and Fe concentrations in a disturbed southern Appalachian high elevation wetland. *Geomicrobiology Journal, 29*(2), 124-138. doi: Doi 10.1080/01490451.2011.558557

Klappenbach, J. A., Dunbar, J. M., & Schmidt, T. M. (2000). rRNA operon copy number reflects ecological strategies of bacteria. *Applied and Environmental Microbiology, 66*(4), 1328-1333. doi: Doi 10.1128/Aem.66.4.1328-1333.2000

Klappenbach, J. A., Saxman, P. R., Cole, J. R., & Schmidt, T. M. (2001). RRNDB: the ribosomal RNA operon copy number database. *Nucleic Acids Research, 29*(1), 181-184. doi: Doi 10.1093/Nar/29.1.181

Koljalg, U., Larsson, K. H., Abarenkov, K., Nilsson, R. H., Alexander, I. J., Eberhardt, U., . . . Ursing, B. M. (2005). UNITE: a database providing web-based methods for the molecular identification of ectomycorrhizal fungi. *New Phytologist, 166*(3), 1063-1068. doi: 10.1111/j.1469-8137.2005.01376.x

Korbie, D. J., & Mattick, J. S. (2008). Touchdown PCR for increased specificity and sensitivity in PCR amplification. *Nature Protocols, 3*(9), 1452-1456.

Kosman, D. J. (2010). Multicopper oxidases: a workshop on copper coordination chemistry, electron transfer, and metallophysiology. *Journal of Biological Inorganic Chemistry, 15*(1), 15-28. doi: DOI 10.1007/s00775-009-0590-9

Lambeth, J. D. (2004). NOX enzymes and the biology of reactive oxygen. *Nature Reviews Immunology, 4*(3), 181-189. doi: Doi 10.1038/Nri1312

Larsen, E. I., Sly, L. I., & McEwan, A. G. (1999). Manganese(II) adsorption and oxidation by whole cells and a membrane fraction of *Pedomicrobium* sp. ACM 3067. *Archives of Microbiology, 171*(257-264).

Lauber, C. L., Strickland, M. S., Bradford, M. A., & Fierer, N. (2008). The influence of soil properties on the structure of bacterial and fungal communities across land-use types. *Soil Biology and Biochemistry, 40*, 2407-2415.

Learman, D. R., Voelker, B. M., Vazquez-Rodriguez, A. I., & Hansel, C. M. (2011a). Formation of manganese oxides by bacterially generated superoxide. *Nature Geoscience, 4*(2), 95-98. doi: Doi 10.1038/Ngeo1055

Learman, D. R., Wankel, S. D., Webb, S. M., Martinez, N., Madden, A. S., & Hansel, C. M. (2011b). Coupled biotic-abiotic mn(II) oxidation pathway mediates the formation and structural evolution of biogenic mn oxides. *Geochimica Et Cosmochimica Acta, 75*(20), 6048-6063. doi: DOI 10.1016/j.gca.2011.07.026

Leinonen, R., Akhtar, R., Birney, E., Bower, L., Cerdeno-Tarraga, A., Cheng, Y., Cleland, I., Faruque, N., Goodgame, N., Gibson, R., Hoad, G., Jang, M., Pakseresht, N., Plaister, S., Radhakrishnan, R., Reddy, K., Sobhany, S., Hoopen, P.T., Vaughan, R., Zalunin,

V., Cochrane, G. (2010). The European Nucleotide Archive. *Nucleic Acids Research.*
1-4.

Li, S., Zhu, T., Liu, G., & Zhu, H. (2012). Diversity of macrofungal community in Bifeng
Gorge: the core giant panda habitat in China. *African Journal of Biotechnology,*
11(8), 1970-1976.

Li, W., & Oyama, S. T. (1998). Mechanism of ozone decomposition on a manganese oxide
catalyst. 2. steady-state and transient kinetic studies. *Journal of the American*
Chemical Society, 120(35), 9047-9052. doi: Doi 10.1021/Ja9814422

Longo, A. V., Rodriguez, D., Leite, D. D., Toledo, L. F., Almeralla, C. M., Burrowes, P. A.,
& Zamudio, K. R. (2013). ITS1 copy number varies among *Batrachochytrium*
dendrobatidis strains: implications for qPCR estimates of infection intensity from
field-collected amphibian skin swabs. *Plos One, 8*(3). doi: ARTN e59499 DOI
10.1371/journal.pone.0059499

Luther, G. W. (2010). The role of one- and two-electron transfer reactions in forming
thermodynamically unstable intermediates as barriers in multi-electron redox
reactions. *Aquatic Geochemistry, 16*(3), 395-420. doi: DOI 10.1007/s10498-009-
9082-3

Manceau, A., Gorshkov, A. I., & Drits, V. A. (1992). Structural chemistry of Mn, Fe, Co, and
Ni in manganese hydrous oxides. 1. information from xanes spectroscopy. *American*
Mineralogist, 77(11-12), 1133-1143.

Manceau, A., Marcus, M. A., & Grangeon, S. (2012). Determination of Mn valence states in
mixed-valent manganates by XANES spectroscopy. *American Mineralogist, 97*(5-6),
816-827. doi: Doi 10.2138/Am.2012.3903

Manceau, A., Marcus, M. A., Grangeon, S., Lanson, M., Lanson, B., Gaillot, A. C., . . . Soderholm, L. (2013). Short-range and long-range order of phyllomanganate nanoparticles determined using high-energy X-ray scattering. *Journal of Applied Crystallography, 46*(1), 193-209. doi: Doi 10.1107/S0021889812047917

Mann, P. J. G., & Quastel, J. H. (1946). Manganese metabolism in soils. *Nature, 158*(4005), 154-156.

Matsumoto, P. S. (2005). Trends in ionization energy of transition-metal elements. *Journal of Chemical Education, 82*(11), 1660-1661.

Mayhew, L. E., Swanner, E. D., Martin, A. P., & Templeton, A. S. (2008). Phylogenetic relationships and functional genes distribution of a gene (mnxG) encoding a putative manganese oxidizing enzyme in *Bacillus* species. *Applied and Environmental Microbiology, 74*(23), 7265-7271.

Minnis, A. M., & Lindner, D. L. (2013). Phylogenetic evaluation of *Geomyces* and allies reveals no close relatives of *Pseudogymnoascus destructans*, comb. nov., in bat hibernacula of eastern North America. *Fungal Biology, 117*(9), 638-649.

Miyata, N., Tani, Y., Iwahori, K., & Soma, M. (2004). Enzymatic formation of manganese oxides by an *Acremonium*-like hyphomycete fungus, strain KR21-2. *Fems Microbiology Ecology, 47*(1), 101-109. doi: Doi 10.1016/S0168-9496(03)00251-4

Nadkarni, M. A., Martin, F. E., Jacques, N. A., & Hunter, N. (2002). Determination of bacterial load by real-time PCR using a broad-range (universal) probe and primers set. *Microbiology-Sgm, 148*, 257-266.

Neilands, J. B. (1995). Siderophores - structure and function of microbial iron transport compounds. *Journal of Biological Chemistry, 270*(45), 26723-26726.

Northup, D. E., Barns, S. M., Yu, L. E., Spilde, M. N., Schelble, R. T., Dano, K. E., . . . Dahm, C. N. (2003). Diverse microbial communities inhabiting ferromanganese deposits in Lechuguilla and Spider caves. *Environmental Microbiology, 5*(11), 1071-1086.

Northup, D. E., Dahm, C. N., Melim, L. A., Spilde, M. N., Crossey, L. J., Lavoie, K. H., . . . Barns, S. M. (2000). Evidence for geomicrobiological interactions in Guadalupe caves. *Journal of Cave and Karst Studies, 62*(2), 80-90.

O'Brien, H. E., Parrent, J. L., Jackson, J. A., Moncalvo, J. M., & Vilgalys, R. (2005). Fungal community analysis by large-scale sequencing of environmental samples. *Applied and Environmental Microbiology, 71*(9), 5544-5550. doi: Doi 10.1128/Aem.71.9.5544-5550.2005

Orgiazzi, A., Bianciotto, V., Bonfante, P., Daghino, S., Ghignone, S., Lazzari, A., . . . Girlanda, M. (2013). 454 Pyrosequencing analysis of fungal assemblages from geographically distant, disparate soils reveals spatial patterning and a core mycobiome. *Diversity, 5*, 73-98.

Parker, D. L., Lee, S. W., Geszvain, K., Davis, R. E., Gruffaz, C., Meyer, J. M., . . . Tebo, B. M. (2014). Pyoverdine synthesis by the Mn(II)-oxidizing bacterium *Pseudomonas putida* GB-1. *Frontiers in Microbiology, 5*.

Parker, D. L., Sposito, G., & Tebo, B. M. (2004). Manganese(III) binding to a pyoverdine siderophore produced by a manganese(II)-oxidizing bacterium. *Geochimica Et Cosmochimica Acta, 68*(23), 4809-4820. doi: DOI 10.1016/j.gca.2004.05.038

Peiris, D., Dunn, W. B., Brown, M., Kell, D. B., Roy, I., & Hedger, J. N. (2008). Metabolite profiles of interacting mycelial fronts differ for pairings of the wood decay

basidiomycete fungus, *Stereum hirsutum* with its competitors *Coprinus micaceus* and *Coprinus disseminatus*. *Metabolomics, 4*, 52-62.

Post, J. E. (1999). Manganese oxide minerals: crystal structures and economic and environmental significance. *Proceedings of the National Academy of Sciences of the United States of America, 96*(7), 3447-3454. doi: DOI 10.1073/pnas.96.7.3447

Post, J. E., & Bish, D. L. (1988). Rietveld refinement of the todorokite structure. *American Mineralogist, 73*(7-8), 861-869.

Post, J. E., Heaney, P. J., & Hanson, J. (2003). Synchrotron x-ray diffraction study of the structure and dehydration behavior of todorokite. *American Mineralogist, 88*(1), 142-150.

Post, J. E., & Veblen, D. R. (1990). Crystal-structure determinations of synthetic sodium, magnesium, and potassium birnessite using tem and the rietveld method. *American Mineralogist, 75*(5-6), 477-489.

Reynolds, H. T., & Barton, H. A. (2014). Comparison of the white-nose syndrome agent *Pseudogymnoascus destructans* to cave-dwelling relatives suggests reduced saprotrophic enzyme activity. *Plos One, 9*(1), e86437.

Santelli, C. M., Pfister, D. H., Lazarus, D., Sun, L., Burgos, W. D., & Hansel, C. M. (2010). Promotion of Mn(II) oxidation and remediation of coal mine drainage in passive treatment systems by diverse fungal and bacterial communities. *Applied and Environmental Microbiology, 76*(14), 4871-4875. doi: Doi 10.1128/Aem.03029-09

Santelli, C. M., Webb, S. M., Dohnalkova, A. C., & Hansel, C. M. (2011). Diversity of Mn oxides produced by Mn(II)-oxidizing fungi. *Geochimica Et Cosmochimica Acta, 75*(10), 2762-2776. doi: DOI 10.1016/j.gca.2011.02.022

Schadt, C. W., Martin, A. P., Lipson, D. A., & Schmidt, S. K. (2003). Seasonal dynamics of previously unknown fungal lineages in tundra soils. *Science, 301*(5638), 1359-1361. doi: DOI 10.1126/science.1086940

Schloss, P. D., Westcott, S. L., Ryabin, T., Hall, J. R., Hartmann, M., Hollister, E. B., . . . Weber, C. F. (2009). Introducing MOTHUR: open-source, platform-independent, community-supported software for describing and comparing microbial communities. *Applied and Environmental Microbiology, 75*(23), 7537-7541. doi: Doi 10.1128/Aem.01541-09

Schmidt, P.-A., Bálint, M., Greshake, B., Bandow, C., Römbke, J., & Schmitt, I. (2013). Illumina metabarcoding of a soil fungal community. *Soil Biology and Biochemistry, 65*, 128-132.

Spilde, M. N., Northup, D. E., Boston, P., Schelble, R., Dano, K., Crossey, L., & Dahm, C. (2005). Geomicrobiology of cave ferromanganese deposits: a field and laboratory investigation. *Geomicrobiology Journal, 22*, 99-116.

Spiro, T. G., Bargar, J. R., Sposito, G., & Tebo, B. M. (2010). Bacteriogenic manganese oxides. *Accounts of Chemical Research, 43*(1), 2-9. doi: Doi 10.1021/Ar800232a

Sunda, W. G., & Kieber, D. J. (1994). Oxidation of humic substances by manganese oxides yields low-molecular-weight organic substrates. *Nature, 367*(6458), 62-64. doi: Doi 10.1038/367062a0

Takemoto, D., Tanaka, A., & Scott, B. (2007). NADPH oxidases in fungi: diverse roles of reactive oxygen species in fungal cellular differentiation. *Fungal Genetics and Biology, 44*(11), 1065-1076. doi: DOI 10.1016/j.fgb.2007.04.011

Tamayo-Ramos, J. A., van Berkel, W. J. H., & de Graaff, L. H. (2012). Biocatalytic potential of laccase-like multicopper oxidases from *Aspergillus niger*. *Microbial cell factories, 11*(165), 1-11.

Tang, Y. Z., Zeiner, C. A., Santelli, C. M., & Hansel, C. M. (2013). Fungal oxidative dissolution of the Mn(II)-bearing mineral rhodochrosite and the role of metabolites in manganese oxide formation. *Environmental Microbiology, 15*(4), 1063-1077. doi: Doi 10.1111/1462-2920.12029

Tani, Y., Miyata, N., Ohashi, M., Ohnuki, T., Seyama, H., Iwahori, K., & Soma, M. (2004). Interaction of inorganic arsenic with biogenic manganese oxide produced by a Mn-oxidizing fungus, strain KR21-2. *Environmental Science & Technology, 38*(24), 6618-6624. doi: Doi 10.1021/Es049226i

Tebo, B. M., Bargar, J. R., Clement, B. G., Dick, G. J., Murray, K. J., Parker, D., . . . Webb, S. M. (2004). Biogenic manganese oxides: properties and mechanisms of formation. *Annual Review of Earth and Planetary Sciences, 32*, 287-328. doi: DOI 10.1146/annurev.earth.32.101802.120213

Tebo, B. M., Johnson, H. A., McCarthy, J. K., & Templeton, A. S. (2005). Geomicrobiology of manganese(II) oxidation. *Trends in Microbiology, 13*(9), 421-428. doi: DOI 10.1016/j.tim.2005.07.009

Templeton, A. S., Staudigel, H., & Tebo, B. M. (2005). Diverse Mn(II)-oxidizing bacteria isolated from submarine basalts at Loihi seamount. *Geomicrobiology Journal, 22*(3-4), 127-139.

Trouwborst, R. E., Clement, B. G., Tebo, B. M., Glazer, B. T., & Luther, G. W., 3rd. (2006). Soluble Mn(III) in suboxic zones. *Science, 313*(5795), 1955-1957. doi: 10.1126/science.1132876

Vanderwolf, K. J., Malloch, D., McAlpine, D. F., & Forbes, G. J. (2013). A world review of fungi, yeasts, and slime molds in caves. *International Journal of Speleology, 42*(1), 77-96.

Vignais, P. V. (2002). The superoxide-generating NADPH oxidase: structural aspects and activation mechanism. *Cellular and Molecular Life Sciences, 59*(9), 1428-1459. doi: DOI 10.1007/s00018-002-8520-9

Vilgalys, R., & Gonzalez, D. (1989). Organization of ribosomal DNA in the basidiomycete *Thanatephorus praticola*. *Current Genetics*. 18:277-280.

Vilgalys, R., & Hester, M. (1990). Rapid genetic identification and mapping of enzymatically amplified ribosomal DNA from several *Cryptococcus* species. *Journal of Bacteriology, 172*, 4238-4246.

Villalobos, M., Lanson, B., Manceau, A., Toner, B., & Sposito, G. (2006). Structural model for the biogenic Mn oxide produced by *Pseudomonas putida*. *American Mineralogist, 91*(4), 489-502.

Vizzini, A., Zotti, M., & Mello, A. (2009). Alien fungal species distribution: the study case of *Flavolashia calocera*. *Biological Invasions, 11*, 417-429.

Webb, S. M., Dick, G. J., Bargar, J. R., & Tebo, B. M. (2005). Evidence for the presence of Mn(III) intermediates in the bacterial oxidation of Mn(II). *Proceedings of the National Academy of Sciences of the United States of America, 102*(15), 5558-5563. doi: DOI 10.1073/pnas.0409119102

Warner, J. R. (1999). The economics of ribosome biosynthesis in yeast. *Trends in Biochemical Sciences, 24*(11), 437-440.

White, W. B., Culver, D. C., Herman, J. S., Kane, T. C., & Mylroie, J. E. (1995). Karst Lands. *American Scientist, 83*(5), 450-459.

White, W. B., Vito, C., & Scheetz, B. E. (2009). The mineralogy and trace element chemistry of black manganese oxide deposits from caves. *Journal of Cave and Karst Studies, 71*(2), 136-143.

Zhang, Z. Q., & Mu, J. (2007). Effect of hydrothermal time, pH, morphology of manganese oxides. *Journal of Dispersion Science and Technology, 28*(5), 793-796. doi: Doi 10.1080/01932690701345828

Zhang, H. S., Zeidler, A. F. B., Song, W., Puccia, C. M., Malc, E., Greenwell, P. W., . . . Argueso, J. L. (2013). Gene copy-number variation in haploid and diploid strains of the yeast *Saccharomyces cerevisiae*. *Genetics, 193*(3), 785-801. doi: DOI 10.1534/genetics.112.146522

Vita

Bryan Thomas Zorn was born in Poughkeepsie, New York on the 13th of September, 1988. He graduated from Asheville-Buncombe Technical Community College in Asheville, NC in 2009, and went on to complete a Bachelor's Degree in Biology with a Minor in Chemistry from Appalachian State University in the Fall of 2011. The following year, he chose to pursue a Master's in the Science of Cell and Molecular Biology with Dr. Suzanna Bräuer, completed in August of 2014.